Original Article

MOLECULAR METABOLISM

Glucagon-like Peptide-1 receptor Tie2+ cells are essential for the cardioprotective actions of liraglutide in mice with experimental myocardial infarction

Brent A. McLean [1], **Chi Kin Wong, M Golam Kabir, Daniel J. Drucker***

ABSTRACT

Objectives: Glucagon-like peptide-1 receptor (GLP-1R) agonists reduce the rates of major cardiovascular events, including myocardial infarction in people with type 2 diabetes, and decrease infarct size while preserving ventricular function in preclinical studies. Nevertheless, the precise cellular sites of GLP-1R expression that mediate the cardioprotective actions of GLP-1 in the setting of ischemic cardiac injury are uncertain.
Methods: Publicly available single cell RNA sequencing (scRNA-seq) datasets on mouse and human heart cells were analyzed for *Glp1r*/*GLP1R* expression. Fluorescent activated cell sorting was used to localize *Glp1r* expression in cell populations from the mouse heart. The importance of endothelial and hematopoietic cells for the cardioprotective response to liraglutide in the setting of acute myocardial infarction (MI) was determined by inactivating the *Glp1r* in Tie2+ cell populations. Cardiac gene expression profiles regulated by liraglutide were examined using RNA-seq to interrogate mouse atria and both infarcted and non-infarcted ventricular tissue after acute coronary artery ligation.
Results: In mice, cardiac *Glp1r* mRNA transcripts were exclusively detected in endocardial cells by scRNA-seq. In contrast, analysis of human heart by scRNA-seq localized *GLP1R* mRNA transcripts to populations of atrial and ventricular cardiomyocytes. Moreover, very low levels of *GIPR*, *GCGR* and *GLP2R* mRNA transcripts were detected in the human heart. Cell sorting and RNA analyses detected cardiac *Glp1r* expression in endothelial cells (ECs) within the atria and ventricle in the ischemic and non-ischemic mouse heart. Transcriptional responses to liraglutide administration were not evident in wild type mouse ventricles following acute MI, however liraglutide differentially regulated genes important for inflammation, cardiac repair, cell proliferation, and angiogenesis in the left atrium, while reducing circulating levels of IL-6 and KC/GRO within hours of acute MI. Inactivation of the *Glp1r* within the Tie2+ cell expression domain encompassing ECs revealed normal cardiac structure and function, glucose homeostasis and body weight in $Glp1r^{Tie2-/-}$ mice. Nevertheless, the cardioprotective actions of liraglutide to reduce infarct size, augment ejection fraction, and improve survival after experimental myocardial infarction (MI), were attenuated in $Glp1r^{Tie2-/-}$ mice.
Conclusions: These findings identify the importance of the murine Tie2+ endothelial cell GLP-1R as a target for the cardioprotective actions of GLP-1R agonists and support the importance of the atrial and ventricular endocardial GLP-1R as key sites of GLP-1 action in the ischemic mouse heart. Hitherto unexplored species-specific differences in cardiac GLP-1R expression challenge the exclusive use of mouse models for understanding the mechanisms of GLP-1 action in the normal and ischemic human heart.

Keywords Heart; Myocardial infarction; Diabetes; Obesity; Peptides; G protein coupled receptors

1. INTRODUCTION

Glucagon-like peptide-1 (GLP-1) is an enteroendocrine peptide that circulates at low levels in the inter-prandial state, with GLP-1 levels rising transiently following food ingestion [1]. GLP-1 acts on pancreatic endocrine cells to control islet hormone release and glucose homeostasis [2]. GLP-1 also acts in the brain to inhibit gastrointestinal motility thereby slowing the rate of nutrient absorption, and communicates signals via the neuronal GLP-1 receptor (GLP-1R) to attenuate appetite, resulting in weight loss with sustained administration of glucagon-like peptide-1 receptor agonists (GLP1RA) [3]. GLP-1 is essential for glucose homeostasis as deletion of the *Gcg* gene encoding GLP-1 from the gut [4], as well as both pharmacological antagonism or genetic inactivation of the GLP-1R [5–7], produces dysregulated islet hormone secretion and glucose intolerance.

The glucoregulatory and anorectic properties of GLP-1 action are conserved in humans, including people with type 2 diabetes (T2D), supporting pharmaceutical development of multiple degradation-resistant short and long-acting GLP-1Rs for the treatment of T2D [2]. GLP-1 R A have proven to be useful agents for therapy of T2D, reducing

Department of Medicine, Lunenfeld-Tanenbaum Research Institute, Mt. Sinai Hospital, University of Toronto, Toronto, ON M6B 3G3, Canada

[1] Current address: Cogent Biosciences, 4840 Pearl E Circle, Suite 100, Boulder, CO 80301.

*Corresponding author. E-mail: drucker@lunenfeld.ca (D.J. Drucker).

Received October 17, 2022 • Revision received November 6, 2022 • Accepted November 9, 2022 • Available online 14 November 2022

https://doi.org/10.1016/j.molmet.2022.101641

glycosylated hemoglobin, while preventing weight gain or promoting weight loss in the majority of treated subjects. Moreover, administration of GLP-1RA at higher doses than those required for glucose-lowering produces substantial weight loss, enabling approval of two different GLP-1RA, liraglutide and semaglutide, for the therapy of obesity [3].

Beyond the control of metabolism, native GLP-1 reduces ischemic injury of the heart in preclinical models through mechanisms requiring the GLP-1R [8,9]. Conversely, mice with germline genetic inactivation of the GLP-1R exhibit exhibited impaired ventricular function in response to hypoglycemia or epinephrine administration [10]. Collectively, these studies highlight the importance of the GLP-1R for the cardiac response to stress or ischemic injury. Moreover, both native GLP-1 and degradation-resistant GLP-1RA reduce cardiac injury and preserve ventricular function in animals and humans [11–15]. Notably, these actions of GLP-1RA are attenuated in preclinical studies by concomitant administration of the GLP-1R antagonist exendin (9–39) [16,17], fostering considerable interest in the mechanisms linking GLP-1R-dependent signaling to cardioprotection.

The translational importance of the cardiovascular actions of GLP-1RA first identified in preclinical studies was bolstered by the results of cardiovascular outcome trials (CVOTs) examining the safety of GLP-1RA in people with T2D with risk factors for, or with established cardiovascular disease. The results of these CVOTs have shown that multiple GLP-1RA are safe to use in people with T2D at high risk for major adverse cardiovascular events (MACE), principally stroke, myocardial infarction, and cardiovascular death [18]. Moreover, structurally distinct long-acting GLP-1RA reduced the rates of MACE [18,19], including, in some trials, a notable reduction in rates of myocardial infarction in people with T2D [20,21].

Despite translation of the cardioprotective actions of GLP-1RA from animals to humans with T2D, the underlying mechanisms and sites of action linking activation of the GLP-1R to protection of the ischemic heart remain incompletely understood [22]. Moreover, the functional importance and contributions of GLP-1Rs within and outside the heart, for reduction of ischemic myocardial injury remains uncertain. We previously demonstrated that GLP-1Rs targeted by myosin heavy chain-Cre were not required for the acute cardioprotective actions of liraglutide in the ischemic mouse heart [23]. Here we investigated the cellular identity of *Glp1r/GLP1R*-expressing cells within the mouse and human heart, localizing *GLP1R* expression to human cardiomyocytes and *Glp1r* in the mouse ventricle, to endocardial endothelial cells. We subsequently used the TEK receptor tyrosine kinase (also known as Tie2) promoter to target the reduction of *Glp1r* expression within endothelial cells, followed by induction of experimental MI in mice treated with or without liraglutide. Our studies demonstrate an important role for Tie2+ GLP-1R+ cells in mediating acute liraglutide-induced cardioprotection, in association with regulation of inflammatory pathways in the mouse atrium.

2. MATERIALS AND METHODS

2.1. Animal housing

All animal procedures were approved by the Animal Care and Use Subcommittee at the Toronto Centre for Phenogenomics (TCP) at the Mount Sinai Hospital (Toronto, Canada). Mice were housed up to five per cage on a 12-h light/dark cycle (7 am–7 pm) at 23 °C, with ad libitum access to water and regular chow diet with 18% kcal from fat (Envigo).

2.2. Animal breeding

C57BL/6 J wildtype mice were obtained from an internal colony bred within TCP. Mice with *Glp1r* deletion under the regulation of the Tie2 gene promoter (*Tek*) were generated by crossing Tg (Tek-Cre)1Ywa mice (Tie2-Cre) (Jackson Laboratory 008863) with $Glp1r^{fl/fl}$ mice, kindly provided by Dr. R. Seeley, University of Michigan [24]. Male mice with a single Tie2-Cre allele and homozygous for $Glp1r^{fl/fl}$ were crossed with female mice homozygous for $Glp1r^{fl/fl}$ mice to produce $Glp1r^{fl/fl}$ ($Glp1r^{Tie2+/+}$) and $Glp1r^{fl/fl}$ /Tie2-Cre ($Glp1r^{Tie2-/-}$).

2.3. Liraglutide treatment

Dosing of liraglutide or saline (vehicle) was administered by subcutaneous injection (S·C.): 75 μg/kg of liraglutide twice daily (BID) in 4 ml/kg volume for 7 days prior to surgical myocardial infarction as previously described [13]. The final dose was administered 1–2 h prior to the surgical procedure.

2.4. Oral glucose tolerance test

For oral glucose tolerance testing, mice were fasted 5 h, and treated with liraglutide, 75 μg/kg, or vehicle at the start of fasting. Oral glucose (Sigma) was administered by gavage at 1.5 g/kg and a concentration of 0.15 g/ml glucose in water. Glucose was measured (Contour glucometer) from tail vein blood taken pre-dose (time 0), 10, 20, 30, 60, 90, and 120 min after glucose gavage.

2.5. Surgical myocardial infarction

Experimental myocardial infarction (MI) was induced via permanent ligation of the left anterior descending (LAD) coronary artery in 10–12-week-old male mice as described previously [13]. Sham-operated mice underwent the same procedure by moving the suture underneath the LAD coronary artery but without tying off the vessel. The surgeon was blinded to the genotypes and treatment for all surgeries. Mice with perioperative mortality on the day of surgery, generally within the first hour reflecting problematic intubation, were excluded from the study. Necropsy of subsequent mortality events consistently revealed evidence for cardiac rupture as indicated by a large blood clot in the thoracic cavity.

2.6. Echocardiography

Echocardiography ultrasound for the assessment of LV function was performed in isoflurane-anesthetized mice (2–3%) (30–40 MHz; Vevo770, VisualSonics) with body temperature maintained on a heated platform and continually monitored via anal probe. The operator was blinded to the genotype and treatment of all mice for ultrasound measurements and subsequent analysis.

2.7. Necropsy

For non-surgical cohorts and 4-week post MI cohorts, mice were euthanized by CO_2 inhalation. Blood was collected by cardiac puncture and mixed with 10% v/v TED (5000 KIU/ml Trasylol, 1.2 mg/ml EDTA, 0.1 nmol/l Diprotin A). Blood was spun at 12,000 g for 5 min for plasma collection. Tissues for RNA analysis were collected by snap freezing in liquid nitrogen. For histology analysis, infarcted hearts were rinsed in phosphate buffered saline (PBS) followed by 1 M KCl to arrest the heart in diastole, followed by fixation in 10% neutral buffered formalin. For 3-hrs post infarcted and sham operated cohorts, mice were euthanized immediately after echocardiography measurements under isoflurane anesthesia.

2.8. Heart sub-region dissection

For isolation of cardiac sub-regions, non-infarcted hearts were rinsed in PBS and a cannula passed through the aorta into the LV. Methylene blue dye (1% w. v. in PBS) was injected into the LV chamber and incubated for 5 min. Subsequently, the heart was cut on the short axis,

rinsed in PBS and frozen in Optimal Cutting Temperature (OCT) medium. With minimal sample thawing, a dissecting microscope was used to scrape endocardial and LV free wall, mid-myocardial samples from cryosection slides for subsequent RNA analysis.

2.9. Fluorescence activated cell sorting (FACS) cytometry

For isolation of cardiac cells, mice were anesthetized with Avertin (intraperitoneal injection: 250 mg/kg or sufficient to cause lack of toe-pinch response). Hearts were perfused via aortic cannulation and cardiomyocyte and non-cardiomyocyte fractions were prepared from adult mouse ventricles as described [25]. Ventricles were digested using 1.5 mg/ml collagenase II (Worthington Biochemicals, Lakewood, NJ; Cat# LS004176). Following sedimentation of isolated cardiomyocytes via centrifugation at 20g for 3 min, the supernatant was collected and centrifuged at 300 g for 5 min to pellet non-cardiomyocytes. Isolated cells were washed with cold FACS buffer (PBS with 2 mM ethylenediaminetetraacetic acid (EDTA), 25 mM ((4-(2-hydroxyethyl)-1-piperazineethanesulfonic acid))HEPES, 2%v/v fetal bovine serum) followed by Fc blocking for 15 min followed by a 30 min incubation with florescent conjugated antibodies. Cells were sorted with a MoFlo Astrios Cell Sorter (Beckman) into FBS-coated tubes, pelleted and frozen for RNA analysis.

2.10. RNA isolation, qPCR

Frozen tissues or cells were homogenized in Tri Reagent (MRC) using a TissueLyser II (Qiagen) followed by RNA purification according to manufacturer directions and precipitation with ethanol. 500–1000 ng total RNA was treated with DNase1 (Thermo Fisher Scientific, EN0521), and cDNA was synthesized using random hexamers and SuperScript III (Thermo Fisher Scientific, 1,808,044). Quantitative PCR used TaqMan Fast Advanced Master Mix (Thermo Fisher), Taqman probes (Supplemental table 1) on a QuantStudio 5 system (Thermo Fisher). Relative gene expression was calculated by the 2-ΔΔCT method using *Ppia* as the reference gene.

2.11. Cytokine measurements

Terminal blood plasma cytokines were measured with the V-PLEX Proinflammatory Panel 1 Mouse Kit (Mesoscale, K15048D) and a 10-cytokine panel for IFN-γ, IL-1β, IL-2, IL-4, IL-5, IL-6, KC/GRO, IL-10, IL-12p70, and TNF-α.

2.12. Bulk RNA sequencing

RNA samples were subjected to bulk RNA sequencing (RNA-seq) as described before [26]. Samples were prepared into mRNA libraries using TruSeq stranded mRNA library preparation kit (Illumina) and sequenced on a NovaSeq (Illumina) with a read length of 2×200 bp. An average of 18 million uniquely mapped reads was obtained per library. Reads were aligned to mm10 using the STAR aligner [27]. Count tables generated were subjected to DESeq2 for differential expression analysis [28] and Webgestalt for gene set enrichment analysis [29]. Differential expression was defined as adjusted p value < 0.05. All raw data and a count table for all samples were deposited into the gene expression omnibus database with the accession number GSE217736.

2.13. Single cell RNA sequencing analysis

The Tabula Muris datasets were used to examine mouse heart *Glp1r* expression [30]. Two published single cell RNA-seq data sets were analyzed for human *GLP1R* expression in the normal and ischemic heart [31,32]. For the mouse datasets, Seurat 4.1.1 was used for the analysis and generation of all plots [33]. For the human datasets, uniform manifold approximation and projection (UMAP) and violin plots were generated using Scanpy 1.9.1 [34].

2.14. Histology

Mice were anesthetized using avertin (250 mg/kg i. p. injection) and the chest cavity was opened following which an apical injection of 1 M KCl arrested the heart in diastole. Perfusion-fixation was achieved using 4% buffered formalin, and hearts were post-fixed in formalin, embedded in paraffin, sectioned at 6 μm, and stained with Masson's Trichrome or hematoxylin and eosin (H&E) as previously described [23,35]. Cardiac morphometry was carried out using Aperio ImageScope Viewer software (Aperio Technologies) and digital planimetry. Infarcted/scarred LV area was calculated as a % of total LV area.

2.15. Statistics

Data were represented as mean ± standard deviation. Student's t tests and two-way ANOVA tests were performed in GraphPad Prism to calculate statistical significance wherever appropriate. Wilcoxon tests corrected for multiple testing were performed in Scanpy to identify *GLP1R* as a marker in ventricular cardiomyocytes from the myogenic region. A two-tailed student's t test was used for comparison between two groups with a single variable of genotype or treatment. For experiments involving variables of both genotype and treatment, a two-way ANOVA was performed and multiple comparison test (Bonferroni's multiple comparison test). $P \leq 0.05$ was considered statistically significant.

3. RESULTS

The GLP-1R has been localized to the atria and ventricles in the mouse and human heart, although the precise cardiac cell types displaying *GLP1R*/*Glp1r* expression remain uncertain [30,36,37]. We interrogated publicly available single cell RNA sequencing (scRNA-seq) datasets to identify the specific cardiac cell types that express *Glp1r*/*GLP1R*. First, we analyzed the mouse heart data generated by the Tabula Muris consortium using FACS coupled with SMART-seq2. This dataset contained major cardiac cell types including cardiomyocytes, fibroblast, endothelial cells, smooth muscle cells, endocardial cells, immune cells, and neurons (Figure 1A,B). Expression of *Glp1r* was restricted to a single cluster annotated to endocardial cells that express *Npr3*; no other populations in the dataset expressed *Glp1r* at an appreciable level (Figure 1C).

Next, we analyzed published human scRNA-seq datasets to compare and contrast *Glp1r*/*GLP1R* expression in the mouse and human heart. We examined two scRNA-seq datasets totaling over 650,000 cells: one covers all major cell types in the adult human heart [31], and another describes the transcriptomes of ventricular cells from subjects with MI [32]. Consistent with previous findings in mice [37], *GLP1R* was expressed primarily in atria of the human heart; however, the expression was attributed to cardiomyocytes (positive for *RYR2*) rather than endothelial cells (Figure 1D,E). Consistent with previous analyses of human cardiac RNA in atria and ventricles using PCR [37], atrial cardiomyocytes expressed higher levels of *GLP1R* than ventricular cardiomyocytes (Figure 1D). These findings are also consistent with the detection of *GLP1R* in the human sinoatrial node by in situ hybridization [37]. Other cardiac cell types, including endothelial cells, expressed very low levels of *GLP1R* (Figure 1D,E). Endocardial endothelial cells, as marked by *NPR3*, did not co-localize with human *GLP1R* expression as seen in mice (Figure 1D,E). Notably, *GLP1R* expression in human ventricular cardiomyocytes was significantly

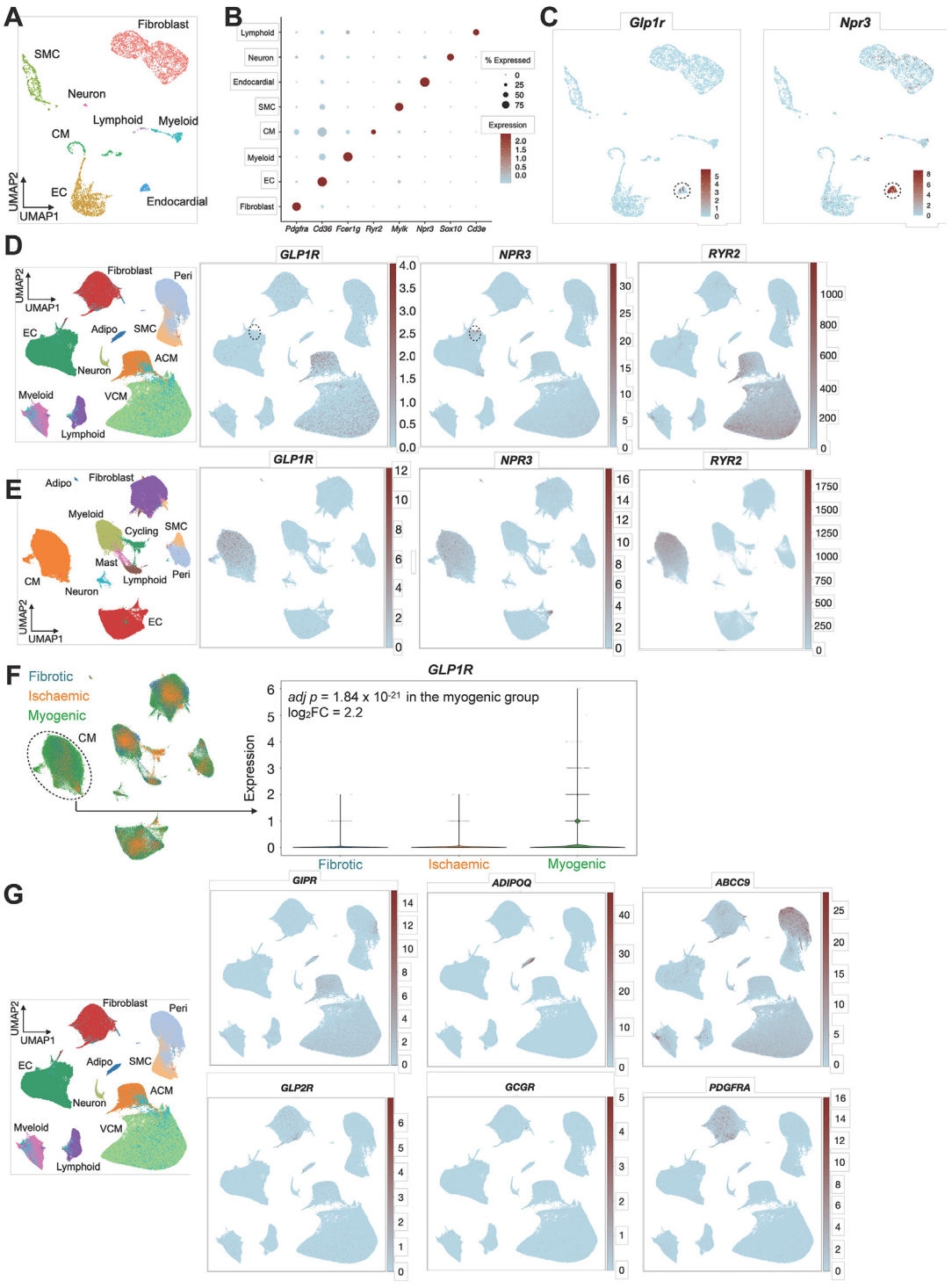

Figure 1: Mouse and human heart *GLP1R* expression analyzed from published single cell RNA sequencing datasets. (A) A UMAP plot showing the annotation of the mouse heart cells from the Tabula Muris scRNA-seq dataset [30]. (B) A dot plot of marker genes specifying each population in the Tabula Muris heart dataset. (C) Expression of *Glp1r* and *Npr3* in various mouse heart cell populations as shown by the Tabula Muris dataset. (D) The dataset from [31] was used for these panels. UMAP plots showing the annotation of the human heart cell atlas (leftmost), followed by expression of *GLP1R*, *NPR3*, and *RYR2* in the dataset. (E) The dataset from [32] was used for these panels. UMAP plots showing the annotation of the ventricular cells from MI subjects (leftmost), followed by expression of *GLP1R*, *NPR3*, and *RYR2* in the dataset. (F) Left: an annotation of the dataset from [32] segregated by conditions of MI. Right: *GLP1R* expression in the ventricular cardiomyocytes segregated by conditions of MI. *GLP1R* was significantly enriched in the myogenic region over other regions as tested by Wilcoxon tests corrected for multiple testing. The conditions of ventricular regions were described as reported [32] and as follows: the myogenic region was the control/unaffected region, the ischemic region was ventricular area affected by recent MI, and the fibrotic region was ventricular area that was healing post—MI. (G) The dataset from [31] was used for these panels. UMAP plots showing the annotation of the human heart cell atlas (leftmost), followed by expression of *GIPR*, *ADIPOQ*, *ABCC9*, *GLP2R*, *GCGR*, and *PDGFRA* in the dataset. Abbreviations: EC: endothelial cell. Adipo: adipocyte. SMC: smooth muscle cell. Peri: pericyte. ACM: atrial cardiomyocyte. VCM: ventricular cardiomyocyte. CM: cardiomyocyte. RYR2: ryanodine receptor 2.

enriched in ventricular cardiomyocytes from the myogenic region as opposed to those from the ischemic or fibrotic regions, suggesting human cardiomyocyte *GLP1R* expression may be perturbed under pathological conditions such as ischemic injury (Figure 1F).

For comparative purposes, we next examined expression of other glucagon-related class B G protein coupled receptors in these human heart datasets. Expression of glucose-dependent insulinotropic peptide receptor (*GIPR*) was detected in three cardiac populations: ventricular and atrial cardiomyocytes (marked by *RYR2* as in Figure 1D), adipocytes (marked by *ADIPOQ*), and pericytes (marked by *ABCC9*) (Figure 1G). Unlike *GLP1R*, expression of *GIPR* in ventricular cardiomyocytes did not differ among myogenic, ischemic, and fibrotic regions (data not shown). Expression of glucagon-like peptide 2 receptor (*GLP2R*) was found in *PDGFRA*-expressing human cardiac fibroblasts (Figure 1G), and some of these cardiac fibroblasts also expressed low levels of the glucagon receptor (*GCGR*) (Figure 1G).

To determine the identity of cell types expressing the *Glp1r* in the mouse cardiac ventricle, the predominant site of ischemic cardiac injury, using techniques independent of RNA-seq, we subjected hearts to enzymatic digestion through perfusion into the coronary arteries. Cardiomyocyte (CM) enriched fractions, whole left ventricle (LV) tissue and grouped whole atria (Atr) tissue were collected. FACS analysis of non-CM LV derived cells was performed to collect major cell types: CD31+ endothelial cells, CD140a+ fibroblasts, CD45 immune cells

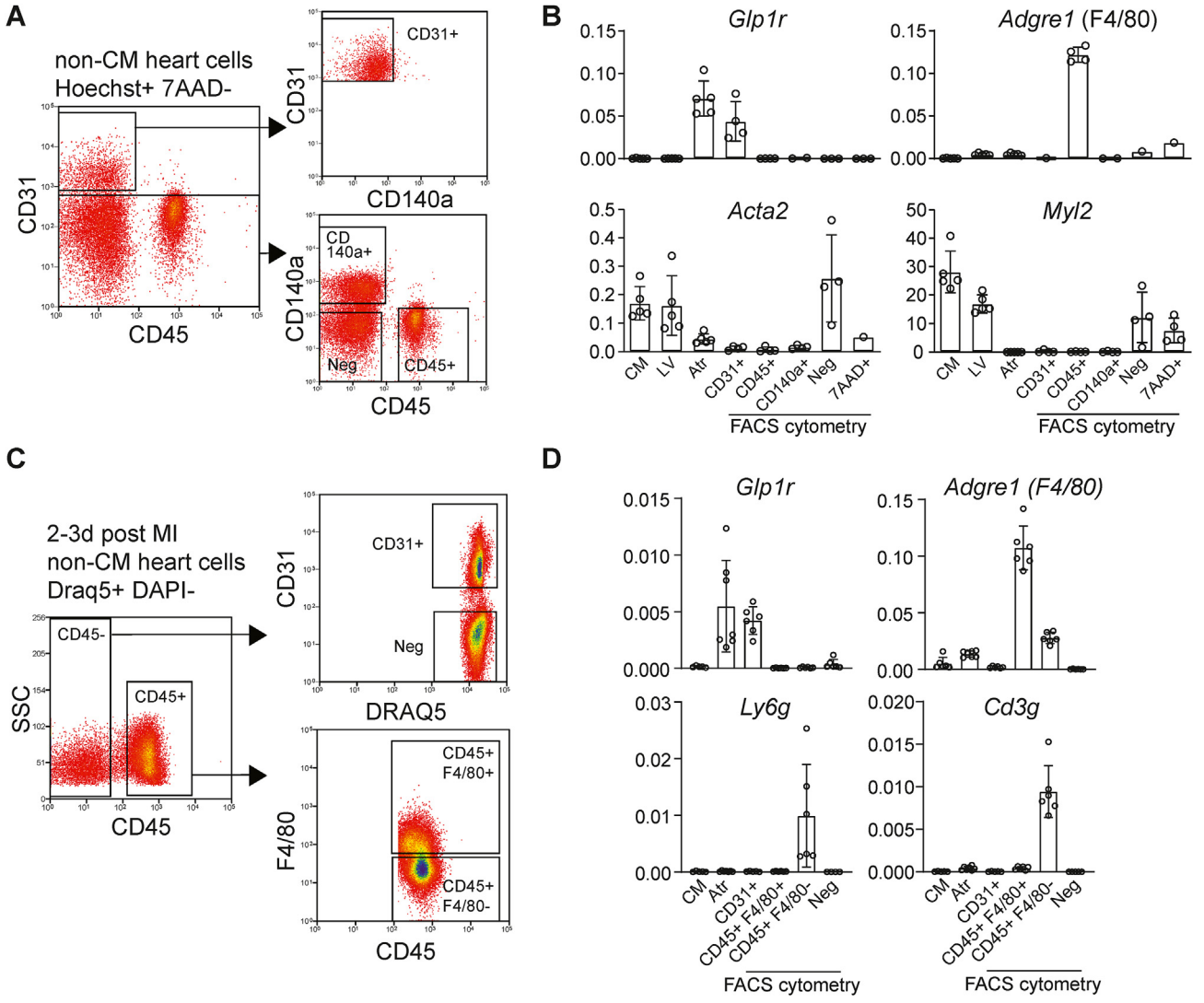

Figure 2: *Glp1r* is enriched in heart ventricle endothelial cells in healthy and infarcted hearts. Ventricular cell suspensions were collected after coronary perfusion, enzymatic digestion of the heart ventricles; (A) Cardiomyocyte (CM) depleted cell fractions (non-CM) were subjected to FACS cytometry, collecting major cell populations: CD31+ (endothelial cells), CD45+ (immune cells), CD140a+ (fibroblasts). Cells negative (Neg) for these markers as well as dead cells staining 7-AAD+ were also collected; Hoechst nuclear staining distinguished cells from debris. (B) Gene expression analysis was performed in FACS collected cells as well as CM enriched fractions, whole left ventricle tissue (LV) and whole atria tissue (Atr) for expression of *Glp1r* and macrophage marker *Adgre1*, smooth muscle marker *Acta2* and ventricular CM marker *Myl2* (n = 4–5). (C) To determine if *Glp1r* positive immune cells are recruited to the heart after myocardial infarction, at 2–3 days after myocardial infarction, hearts were subjected to perfusion digestion as above, with non-CM fractions first gated as nucleus positive (Draq5+), live (DAPI-) and stained for CD31+, CD45+ cells subdivided as F4/80+/− (macrophage marker) and remaining negative stained cells (Neg). (D) Gene expression analysis was performed for *Glp1r*, and marker genes *Adgre1*, neutrophil marker *Ly6g* and T-cell marker *Cd3g* (n = 6). Gene expression values are relative to *Ppia*.

and cells negative (Neg) for CD31, CD140a and CD45 (Figure 2A). Additionally, dead/dying cells positive for 7-AAD were collected for completeness. *Glp1r* expression in FACS collected cells was enriched only in CD31+ endothelial populations (Figure 2B); *Acta2* and *Myl2* are markers for vascular smooth muscle and ventricular myocytes, respectively (Figure 2B). To investigate the possibility that *Glp1r*+ immune cells may localize to the heart following myocardial infarction, we performed FACS on non-CM ventricular cells from hearts 2–3 days post myocardial infarction surgery. We subdivided CD45+ immune cells with the macrophage marker F4/80. Expression of macrophage, neutrophil and T-cell markers *Adgre1*, *Ly6g* and *Cd3g* were enriched in the expected fractions, but only CD31+ endothelial fractions were enriched for *Glp1r* (Figure 2C,D).

As *Glp1r* promoter-directed transgenic reporter expression was detected within a few endothelial cells localized to the mouse endocardium [38], we next assessed the localization of endogenous *Glp1r* mRNA transcripts within endothelial cells of the cardiac endocardium by FACS. We utilized markers for endocardial endothelial cells (EEC)

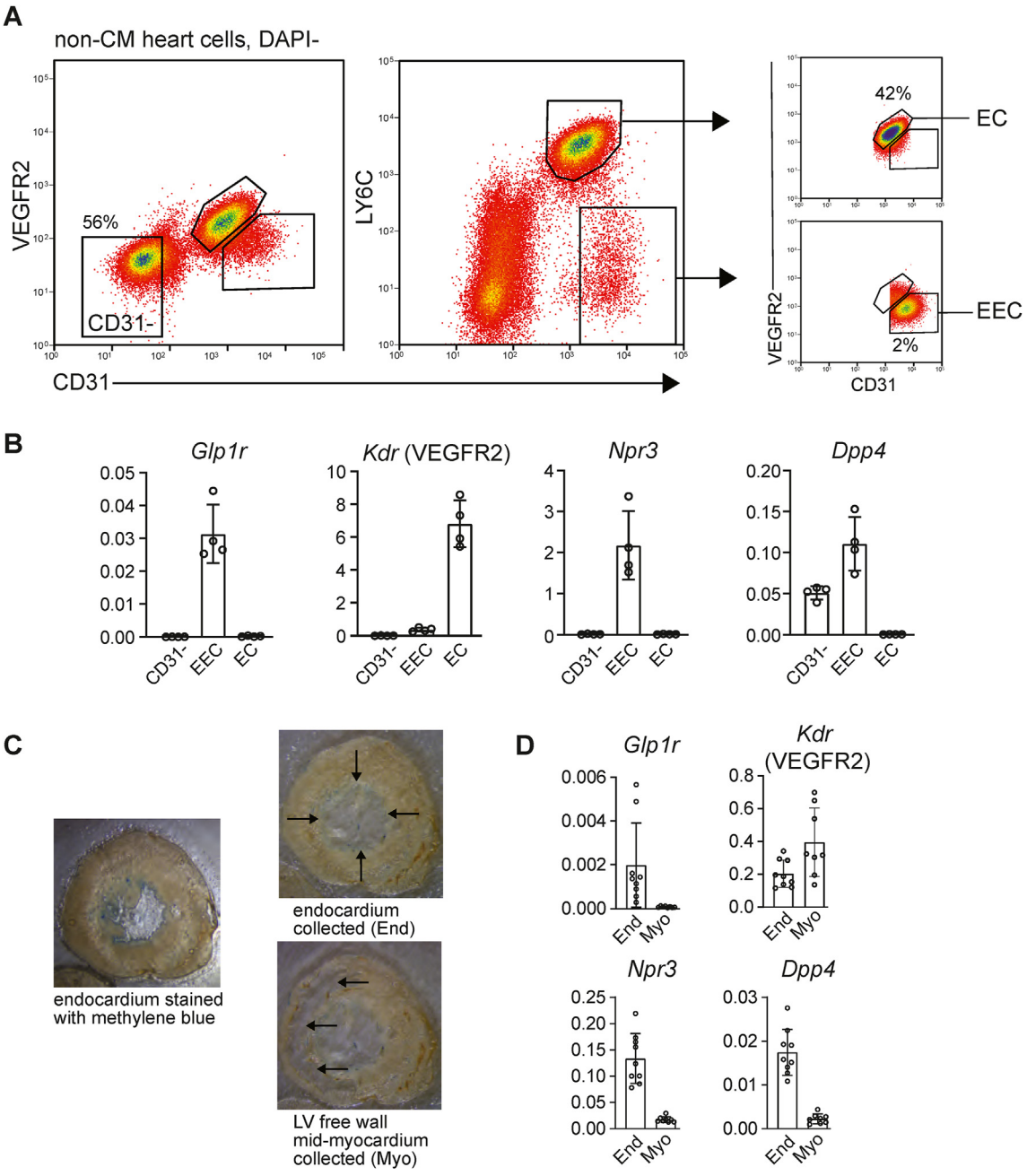

Figure 3: *Glp1r* expression is localized to mouse endocardial endothelial cells. Ventricular endothelial cells were subdivided by FACS cytometry: (A) CD31-cells were collected in addition to CD31+ cells subdivided by markers for endocardial endothelial cells (EEC) VEGFR2^{low}, LY6C^{low} and CD31^{hi}, and remaining ventricular endothelial cells (EC) VEGFR2^{hi}, LY6C^{hi}, CD31^{med}. (B) Gene expression analysis of FACS collected cells for *Glp1r*, marker genes *Kdr* and *Npr3*, and *Dpp4* (n = 4). (C) Hearts with LV chamber stained with methylene blue were cryosectioned and blue endocardium (End) and LV free wall, mid-myocardium (Myo) was collected. Gene expression from dissected cryosections was performed for *Glp1r*, *Kdr*, *Npr3* and *Dpp4* (n = 9). Gene expression values are relative to *Ppia*.

VEGFR2^{low}, LY6C^{low} and CD31^{hi}, and remaining ventricular endothelial cells (EC) VEGFR2^{hi}, LY6C^{hi}, CD31^{med} (Figure 3A) to probe cell fractions for *Glp1r* expression [39]. qPCR detected *Glp1r* mRNA transcripts within ventricular endocardial endothelial cells, consistent with relative enrichment of *Npr3* [40] and *Dpp4* [41] in the same fractions (Figure 3B). We next stained mouse LV chambers with methylene blue to identify endocardium (End; stained blue) and LV free wall, mid-myocardium (Myo; unstained) for anatomical isolation and analysis of gene expression (Figure 3C). Consistent with the data from FACS, *Glp1r*, *Npr3*, and *Dpp4* but not *Kdr* (encoding VEGFR2) mRNA transcripts were enriched in the endocardium, relative to the myocardium (Figure 3D). Together with the Tabula Muris data described above, *Glp1r* expression in the mouse heart is highly enriched within endocardial cells.

To determine the potential mechanisms and pathways regulated by liraglutide in the mouse heart, we performed bulk RNA sequencing (RNA-seq) on the infarcted and non-infarcted regions of the left ventricle, as well as the left and right atrium, isolated from C57BL/6 J mice 3 days after induction of experimental MI. The transcriptomes of each heart region segregated into its own group. Liraglutide did not grossly affect the transcriptome of any of these regions, as shown by the principal component analysis (Figure 4A). Surprisingly, liraglutide treatment did not result in differential expression of genes in the infarcted or non-infarcted regions of the left ventricle (Figure 4B). In contrast, 266 genes were differentially expressed in the atria of liraglutide-treated mice with MI, with 78 genes downregulated and 188 genes upregulated (Figure 4B; Supplemental Table 2). Gene set enrichment analysis for Kyoto Encyclopedia of Genes and Genomes (KEGG) pathways on these differentially expressed genes categorized them broadly into pathways denoting immune function regulation, which were negatively enriched; and pathways in endoplasmic reticulum stress, which were positively enriched (Figure 4C).

We verified the two mostly significantly enriched KEGG pathways, (1) "Cytokine-cytokine receptor interaction" and (2) "Protein processing in endoplasmic reticulum", with a heat map showing that these two terms encompassed atrial genes most significantly altered in response to liraglutide (Figure 4D). Genes associated with the pathway "Cytokine-cytokine receptor interaction" include various chemokines (*Cxcl2*, *Cxcl3*, *Ccl4*), cytokines (*Il6*, *Lif*, *Osm*), and myeloid markers (*Cd14*, *Tlr2*, *Thbd*) (Figure 4D; Supplemental Table 2). Liraglutide also induced numerous genes encoding heat shock proteins (*Hspa1a*, *Hspa1b*, *Hspa1l*, *Dnaja1*, *Dnajb1*) and structural proteins (*Flnc, Myl2, Myh7b, Acta1*) in the atria (Figure 4D; Supplemental Table 2). Although many of these genes were potently upregulated in infarcted LV as compared to non-infarcted LV, liraglutide only modified their expression in atria (Figure 4D).

To replicate the apparent anti-inflammatory effect of liraglutide on atrial gene expression, we performed qPCR on independent cohorts of liraglutide-treated animals to validate the findings of differentially expressed genes identified from the RNA-seq experiments. Liraglutide downregulated the atrial expression of *Cd14*, *Thbd* (thrombomodulin), and *Nfkb1*, while upregulating *Flnc* (Filamin C, Figure 4E). Similarly, liraglutide down-regulated levels of inflammation- and tissue injury-related genes such as *Tlr2*, *Osm*, *Lif*, *Has1*, and *Cxcl3* (Figure 4E). *Il6* was down-regulated in both the LV and LA (Figure 4F). To assess whether the putative ant-inflammatory actions of liraglutide were evident beyond cardiac tissue, we measured levels of a number of cytokines in peripheral blood. Notably, circulating levels of IL-6 and Keratinocyte chemoattractant (KC)/human growth-regulated oncogene (KC/GRO) were reduced 3 h after induction of myocardial infarction in liraglutide-treated mice (Figure 4G).

Given the localization of *Glp1r* expression to mouse cardiac endocardial endothelial cells, we next ascertained the suitability of using *Glp1r*$^{Tie2-/-}$ mice for functional analysis of the importance of the cardiac endothelial *Glp1r*+ cell population. We first assessed *Glp1r* expression in different tissues of *Glp1r*$^{Tie2-/-}$ mice previously generated in our laboratory [42]. Levels of *Glp1r* were modestly reduced in Brunner's glands, an abundant site of *Glp1r* expression, and virtually extinguished in the mouse lung and heart (Figure 5A). Moreover, levels of *Glp1r* were markedly reduced in the LV (Figure 5A). Echocardiographic assessment of basal cardiac function revealed normal ejection fraction, heart rate and LV dimensions in *Glp1r*$^{Tie2+/+}$ vs. *Glp1r*$^{Tie2-/-}$ mice (Figure 5B). Moreover, metabolic assessment of glucose tolerance and body weight revealed no genotype differences, and similar improvements in glucose tolerance and reductions in body weight were detected following liraglutide administration in chow-fed *Glp1r*$^{Tie2+/+}$ vs. *Glp1r*$^{Tie2-/-}$ mice (Figure 5C,D). Hence, *Glp1r*$^{Tie2-/-}$ mice do not exhibit physiological perturbations in cardiac structure, energy homeostasis, and the acute metabolic response to liraglutide. We next ascertained whether the acute cardioprotective actions of liraglutide in mice with coronary artery ligation-induced myocardial ischemia were preserved in *Glp1r*$^{Tie2-/-}$ mice. Consistent with previous findings [13,23], liraglutide increased the survival of *Glp1r*$^{Tie2+/+}$ mice with acute myocardial infarction (Figure 6A). In contrast, liraglutide failed to increase the survival of *Glp1r*$^{Tie2-/-}$ mice with ischemic cardiac injury (Figure 6A). In keeping with these observations, the ejection fraction was increased in liraglutide-treated *Glp1r*$^{Tie2-/-}$ mice but not in *Glp1r*$^{Tie2-/-}$ mice, when assessed 28 days following coronary artery ligation (Figure 6B). Moreover, left ventricular infarct area was reduced in liraglutide-treated *1r*$^{Tie2+/+}$ mice but not in *Glp1r*$^{Tie2-/-}$ mice (Figure 6C,D). These data reveal the dependence of liraglutide on haematopoietic and endothelial GLP-1Rs within the Tie2+ expression domain for its acute cardioprotective effects in mice with ischemic myocardial injury.

4. DISCUSSION

Here we studied the distribution of expression of cardiac GLP-1R mRNA transcripts, localizing *GLP1R* mRNA to human atrial and ventricular cardiomyocytes, and *Glp1r* mRNA to mouse endocardial endothelial cells. Functionally, we observed that the GLP-1RA liraglutide predominantly regulated atrial, rather than ventricular gene expression, in the normal or ischemic mouse heart. Moreover, the acute cardioprotective actions of liraglutide were attenuated in mice with genetic ablation of endothelial cell *Glp1r* expression. These findings extend our understanding of the acute cardioprotective actions of GLP-1RA in the ischemic mouse heart, and highlight species-specific differences in cellular localization of cardiac GLP-1R expression.

Assignment of mechanisms linking native GLP-1 to cardioprotection is challenged by observations that native GLP-1 and GLP-1 metabolites may act through GLP-1R-independent pathways to regulate endothelial and mitochondrial activity in the setting of acute cardiovascular injury [43–45]. Nevertheless, the majority of degradation-resistant GLP-1RA utilized clinically do not generate the identical spectrum of GLP-1 metabolites and are unlikely to activate non-canonical pathways linked to engagement of soluble adenylate cyclase and mitochondrial substrate metabolism [45]. Moreover, the major cardiovascular actions of GLP-1RA, including control of heart rate, blood pressure, and plasma lipids, are mediated via the canonical GLP-1R, and are markedly attenuated in *Glp1r*$^{-/-}$ mice treated with multiple GLP-1RA [36,46,47]. Consistent with the acute studies presented here, we previously demonstrated that *Glp1r*$^{Tie2-/-}$ mice retain normal metabolic

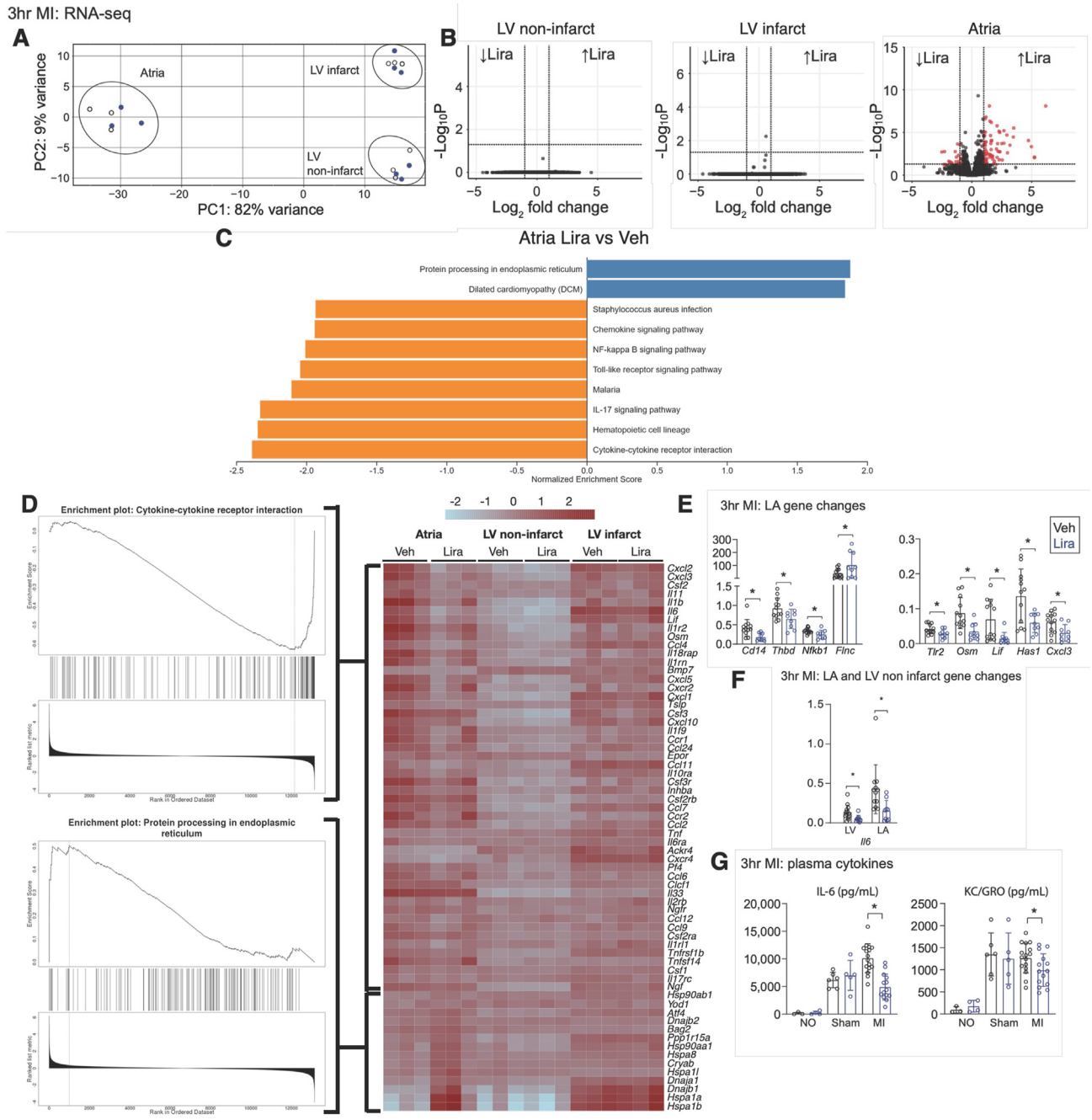

Figure 4: Effects of Liraglutide treatment at 3 h post myocardial infarction. 7 day pre-treatment (B.I.D. 75 μg/kg Liraglutide (Lira) or vehicle (Veh)) was performed and tissue from left ventricle (LV) infarct and non-infarct regions, and pooled left and right atria was collected 3 h s after myocardial infarction for analysis by RNA sequencing (RNA-seq). (A) Principal component analysis demonstrates global transcriptional differences between LV infarct, LV non-infarct and atria. (B) Volcano plots show differentially gene expression in atria but not in LV infarct or LV non-infarct. Upward arrows denote genes upregulated in the Lira group and downward arrows denote genes downregulated in the Lira group. (C) Gene set enrichment analysis reveals significant negative enrichment for KEGG pathways in cytokine and immune functions and positive enrichment for KEGG pathways for endoplasmic reticulum stress. (D) A heat map showing all differentially expressed atrial genes significantly enriched in the KEGG pathways 1) "Cytokine-cytokine receptor interaction" and 2) "Protein processing in endoplasmic reticulum". The expression was ranked from most downregulated (the top) to most upregulated (the bottom). The genes corresponding to their KEGG pathway were bracketed, and an enrichment plot showing the enrichment score for the pathway was shown. LV non-infarct and LV infarct were also shown to demonstrate the specific effect of Lira in atria. (E and F) In new cohorts of mice, qPCR was used to confirm Lira effects seen in RNA-seq, with left atria (LA) and right atria (RA) collected separately. Genes in LA that are significantly changed by Lira. (G) Blood plasma was collected and analyzed for cytokines IL-6 and KC/GRO (n = 9–12).

responses to GLP-1RA, including reduction of lipids and atherosclerosis, with chronic administration of semaglutide [42].

Multiple studies demonstrate that structurally distinct GLP-1RA produce acute cardioprotection in the ischemic mouse and rat heart, findings generally sensitive to blockade with GLP-1R antagonists such as exendin (9–39) [22,48]. Intriguingly, N-terminally truncated and C-terminal fragments of the native GLP-1 peptide also generate acute cardioprotection, independent of the canonical GLP-1R by acting

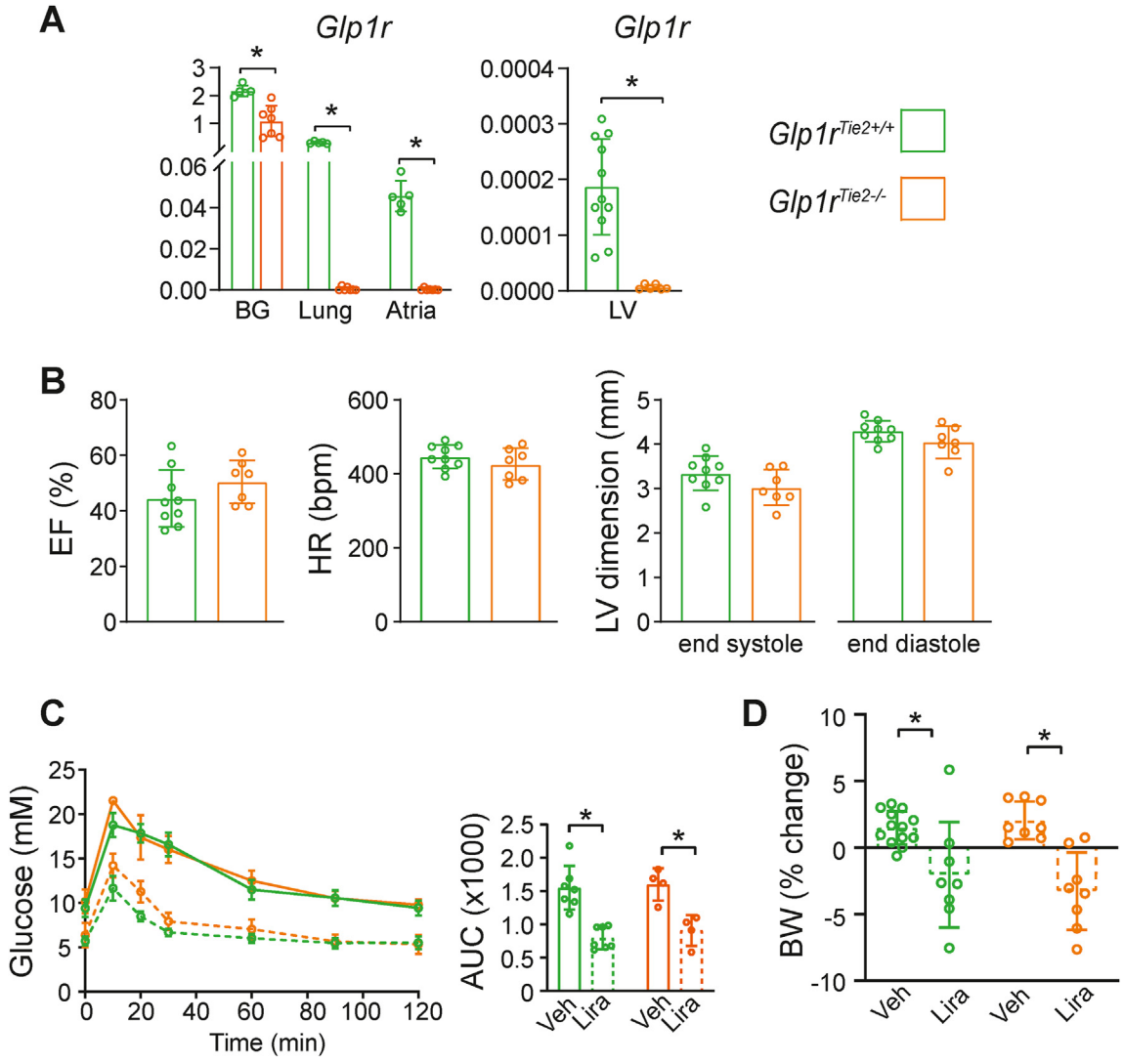

Figure 5: Tie2-Cre targeted Cre recombinase eliminates *Glp1r mRNA* from the heart. (A) Gene expression for *Glp1r* for $Glp1r^{Tie2+/+}$ vs. $Glp1r^{Tie2-/-}$ mice in Brunner's gland (BG), lung, heart atria (n = 5–7) and left ventricle (LV) (n = 9–11). (B) Echocardiography was used to measure LV ejection fraction (EF), heart rate (HR) and LV chamber dimension at end systole and end diastole (n = 7–9). After 3 days of 75 μg/kg Liraglutide B.I.D., (C) oral glucose tolerance (n = 4–7) and (D) bodyweight change (n = 8–13).

through mitochondrial pathways [43–45]. Nevertheless, exendin-4-based GLP-1RA such as exenatide and efpeglenatide reduce MACE events in human CVOTs, yet do not give rise to C-terminal cleavage products identical to those within the native GLP-1 sequence [21,49]. Moreover, the cardioprotective gene expression profile induced by liraglutide in the mouse heart is abolished in $Glp1r^{-/-}$ mice [13]. Collectively these findings favor an important role for the canonical GLP-1R in transducing the cardioprotective actions of GLP-1RA.

The available data suggests that GLP-1Rs localized to the atria are functionally important for the increase in heart rate in mice, rats, and humans treated with GLP-1RA [50,51], findings reflecting simultaneous engagement of GLP-1Rs within the autonomic nervous system and the sinoatrial node. The importance of cardiac GLP-1Rs was further revealed by a reduction in basal heart rate and attenuation of the chronotropic actions of liraglutide in $Glp1r^{CM-/-}$ mice with reduction of atrial *Glp1r* expression [23,46]. Surprisingly however, targeting of the putative GLP-1Rs within cardiomyocytes using myosin heavy chain-Cre did not attenuate the cardioprotective actions of liraglutide in mice with experimental MI [23]. Collectively these findings suggested the importance of non-cardiomyocyte GLP-1R+ cell types for GLP-1R-dependent cardioprotection.

Consistent with the importance of non-cardiomyocyte GLP-1Rs in the mouse heart, here we further localized GLP-1Rs to CD31+ endocardial endothelial cells in the normal and ischemic mouse ventricle and atria. Previous studies using the *Cdh5*-Cre mouse to target endothelial and a subset of hematopoietic lineage cells highlighted the importance of GLP-1R+ endothelial cells, and not immune cells, for the vasoprotective actions of GLP1RA in mice with angiotensin II-induced hypertension [52]. Similarly, we did not detect *Glp1r* expression within immune cells or fibroblasts isolated from the ventricles, either prior to or after experimental MI. Consistent with the importance of endothelial cells as the predominant cell type responsible for murine cardiac *Glp1r* expression, both atrial and ventricular *Glp1r* expression was markedly attenuated in hearts from $Glp1r^{Tie2-/-}$ mice. Nevertheless, basal cardiac structure and function was not different in $Glp1r^{Tie2+/+}$ *vs.* $Glp1r^{Tie2-/-}$ mice. However, the cardioprotective actions of liraglutide to reduce infarct size, augment ejection fraction, and enhance survival, were attenuated in

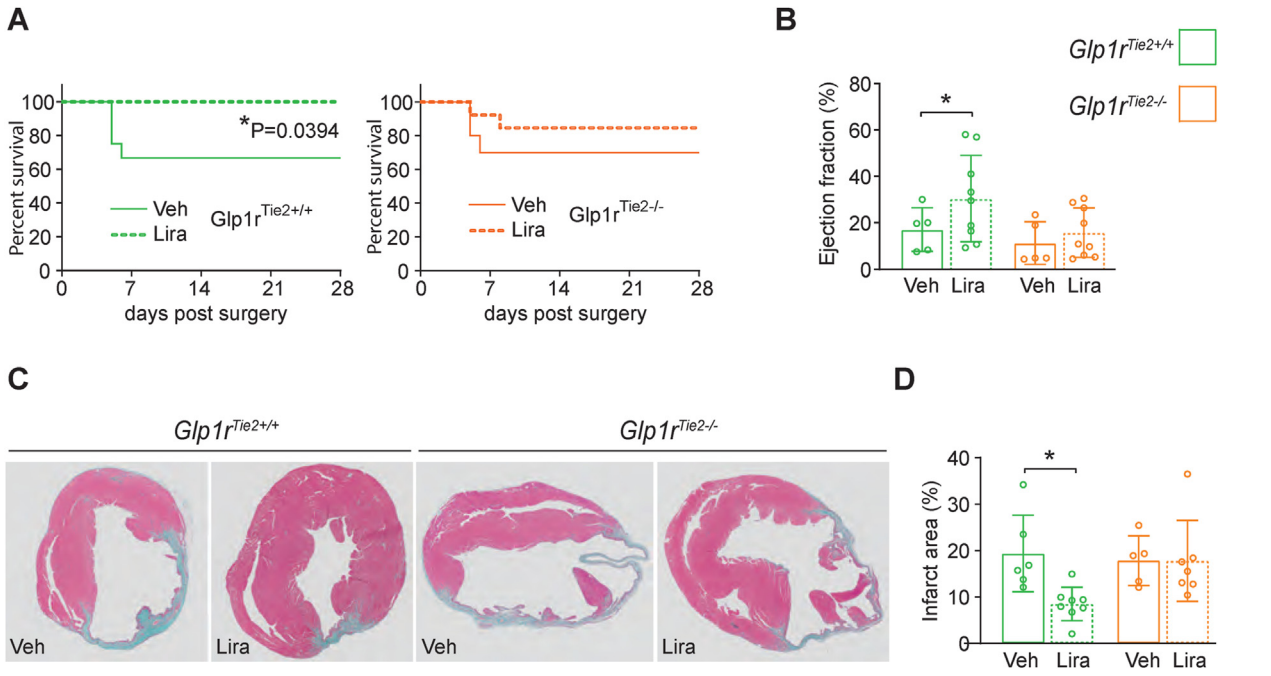

Figure 6: The protective effect of Liraglutide pretreatment in MI is lost in *Glp1r*$^{Tie2-/-}$ mice. Glp1r$^{Tie2+/+}$ and Glp1r$^{Tie2-/-}$ mice were treated 7 days, 75 μg/kg B·I.D. with Liraglutide (Lira) or vehicle (Veh) before surgical myocardial infarction and 28-day follow-up. (A) Post myocardial infarction survival was monitored for 28 days. For the Kaplan Meier survival plots depicted, n = 12 and 11 for saline vs. liraglutide-treated wild type control floxed *Glp1r*$^{Tie2+/+}$mice (left panel), P = .0394 for differences in survival favoring liraglutide. For the Kaplan Meier plot depicting the MI experiment in *Glp1r*$^{Tie2-/-}$ mice, n = 10 vs. 13 for saline vs. liraglutide-treated mice (right panel) P = 0.39. (B) Echocardiography was used to measure left ventricle ejection fraction at day 28. (C) Representative cross sectional images stained with Masson trichrome. (D) Infarct area as percentage of total cross sectional area (n = 5–9).

Glp1r$^{Tie2-/-}$ mice subjected to coronary artery occlusion and experimental MI. Collectively, these findings establish a contributory role for GLP-1R+ cells within the Tie2 cellular expression domain in transducing the cardioprotective actions of GLP-1RA.

Although sometimes overlooked, the endocardium, described here as a major site of murine ventricular endothelial GLP-1R expression, exhibits substantial structural and functional responses to acute myocardial infarction, including extensive inflammatory changes characterized by leukocyte infiltration [53]. Our detection of *Glp1r* mRNA transcripts within mouse endocardial endothelial cells is consistent with localization of scattered cells within the cardiac endocardium in transgenic mice expressing a fluorescent reporter gene under the control of endogenous *Glp1r* regulatory sequences [38]. Intriguingly, sprouting of endocardial endothelial cells in response to acute ischemic myocardial injury has been described in mice, positioning the endocardial endothelium as a potential source of new blood vessels supporting cardiac repair and regeneration [39]. Consistent with these findings, lineage tracing studies identify the endocardium as an important source for new blood vessel formation and neovascularization in the mouse heart after experimental MI induced by coronary artery ligation [54]. Hence the putative functional importance of GLP-1R activity within endothelial cells of the normal and injured myocardium requires greater scrutiny.

Remarkably, despite a large body of evidence from animal and human studies that GLP-1RA preserve ventricular function and reduce the extent of MI within the left ventricle [12,13,55,56], our bulk RNA-seq analyses detected very few differentially expressed mRNA transcripts in the infarcted region or non-infarcted zone of mouse left ventricular tissue following liraglutide administration in mice subjected to experimental MI. In contrast, liraglutide produced substantial changes in the expression of a subset of genes important for the control of inflammation in the mouse atria, consistent with the known anti-inflammatory actions of GLP-1RA in multiple tissues [57], including the normal and injured heart [14,57,58]. Although the left ventricle is a major focus for understanding the cardiac pathophysiology of ischemic myocardial infarction, multiple structural, functional and metabolic changes, are also detectable in the ischemic atria and thought to contribute to the pathophysiology of ischemic myocardial injury [59,60].

Evidence for atrial inflammation in the context of ischemic myocardial infarction has been detected in both animals and humans, generally associated with infiltration of immune cells, including macrophages, lymphocytes and neutrophils, and upregulation of cytokine mRNA transcripts, including *Il1b* and *Tnf* [61,62]. Moreover, circulating levels of biomarkers of inflammation, such as C reactive protein, when measured within 24 h of symptom onset, correlate with the subsequent development of atrial fibrillation in people with myocardial infarction [63]. Our current data extends the anti-inflammatory actions of GLP-1RA such as liraglutide to the atria post infarction. Indeed, we detected reduction of *Cd14*, *Thbd*, *Nfkb1*, *Tlr2*, *Osm*, *Has1* and *Cxcl3* mRNA transcripts, genes associated with immune cells, thrombosis, inflammatory pathways, cell homing and proliferation, migration and differentiation, and vascularization, processes collectively important for the normal and pathological response to acute myocardial injury.

Targeting of inflammation represents a promising strategy to limit the development of cardiovascular disease, including myocardial infarction, in humans. Indeed, administration of canakinumab to immunoneutralize interleukin-1β in people with a previous history of MI and elevated levels of C reactive protein, reduced the rates of MACE, including MI, findings correlated with decreased circulating biomarkers of inflammation [64]. Similarly, emerging data using agents to immunoneutralize interleukin-6

(IL-6) or block the IL-6 receptor suggests that reduction of IL-6 receptor activity in the context of acute MI may preserve myocardium and attenuate the severity of experimental and clinical MI [65,66]. Intriguingly, we detected a reduction in IL-6 expression within the left ventricle and left atria within 3 h of acute myocardial infarction in liraglutide-treated mice. Moreover, circulating levels of IL-6 and KC/GRO were similarly reduced after liraglutide administration when assessed 3 h post MI. Collectively, these findings support the hypothesis that reduction of inflammation through administration of GLP-1RA may contribute to the cardioprotective actions of GLP-1RA, findings that merit further evaluation in both animal and human studies.

In contrast to the importance of the endothelial cell for cardiac GLP-1R expression and function in mice, we were unable to corroborate these findings in scRNA-seq analysis of *GLP1R* expression in the normal and ischemic human heart. Importantly, the relative predominance of atrial vs. ventricular *Glp1r*/*GLP1R* expression remains evident in both the human and mouse heart. Interestingly, the available human RNA-seq evidence suggests that *GLP1R* expression may be less abundant within injured (ischemic and fibrotic) cardiomyocytes, findings that require confirmation in larger studies. Taken together, although the sinoatrial GLP-1R seems to be functionally important in both the mouse and human heart, the relative predominance of *Glp1r* expression in murine endocardial cells vs. *GLP1R* expression in atrial and ventricular cardiomyocytes highlights unexpected species-specific differences in the biology of cardiac GLP-1R expression. Consistent with these species-specific findings for the GLP-1R, the cardiac expression of the *Gcgr* in the mouse heart appears much more abundant [67] relative to the low level expression of *GCGR* mRNA transcripts in the adult human heart [37].

5. CONCLUSIONS AND LIMITATIONS

Here we demonstrate that a substantial proportion of GLP-1R expression in the mouse heart is localized to endocardial endothelial cells. Moreover, a population of GLP-1R+ cells within the Tie2+ domain is essential for an optimal cardioprotective response to GLP-1RA in mice with acute coronary artery ligation and ischemic myocardial injury. Notably, our data has several limitations. First, analysis of *GLP1R* expression using scRNA-seq is limited by the low sensitivity of detection for RNA transcripts expressed at very low levels. Endocardial endothelial cells were significantly underrepresented in the human scRNA-seq datasets and the low number of cells in these data hindered an accurate detection of *GLP1R* in these cells. Second, we did not analyze GLP-1R protein expression, which might differ from RNA expression, and there is limited data available describing GLP-1R protein localization in the mouse or human heart. Third, we studied male mice, and it will be important to examine for possible sex-specific differences in cardiac GLP-1R biology in future studies. Fourth, we studied GLP-1R expression in healthy mouse hearts, and it is possible that cardiac *Glp1r* expression and functional GLP-1R-dependent responses in mice and humans may be modulated by the development of aging, insulin resistance, diabetes, or obesity. Taken together, our findings highlight the potential contributions of cardiac endothelial GLP-1R+ cells for ischemic protection in response to GLP-1RA administration in mice, and emphasize the importance of understanding species-specific differences in cellular localization of GLP-1R expression in the heart.

DUALITY OF INTERESTS

Dr. Drucker has served as a consultant or speaker within the past 12 months to Altimmune Inc, Amgen Inc, AMT Inc, Eli Lilly Inc., Kallyope, Merck Research Laboratories, Novo Nordisk Inc., and Pfizer Inc. Neither Dr. Drucker or his family members hold issued stock directly or indirectly in any of these companies. DJD holds non-exercised options in Kallyope. BAM became an employee of Cogent Biosciences after completion of these studies. GK and CKW have no relevant disclosures

FUNDING

BAM was supported by a fellowship from the Canadian Institutes for Health Research. This work was supported by CIHR grant 154321, investigator initiated funding to DJD/Sinai Health from Novo Nordisk Inc, a Banting and Best Diabetes Centre-Novo Nordisk Chair, and a Sinai Health-Novo Nordisk Foundation Fund in regulatory peptides, to DJD.

AUTHOR CONTRIBUTIONS

BAM conceived and executed the experiments and wrote the paper. CKW and MGK executed experiments and edited the paper. DJD conceived the experiments, reviewed the data and wrote the paper.

CONFLICT OF INTEREST

See Duality of interests.

DATA AVAILABILITY

Data will be made available on request.

APPENDIX A. SUPPLEMENTARY DATA

Supplementary data to this article can be found online at https://doi.org/10.1016/j.molmet.2022.101641.

REFERENCES

[1] Muller TD, Finan B, Bloom SR, D'Alessio D, Drucker DJ, Flatt PR, et al. Glucagon-like peptide 1 (GLP-1). Mol Metabol 2019:3072–130.
[2] Drucker DJ, Habener JF, Holst JJ. Discovery, characterization, and clinical development of the glucagon-like peptides. J Clin Invest 2017;127(12):4217–27.
[3] Drucker DJ. GLP-1 physiology informs the pharmacotherapy of obesity. Mol Metabol 2022;57101351.
[4] Song Y, Koehler JA, Baggio LL, Powers AC, Sandoval DA, Drucker DJ. Gut-proglucagon-derived peptides are essential for regulating glucose homeostasis in mice. Cell Metabol 2019;30(5):976–986 e973.
[5] Scrocchi LA, Brown TJ, MacLusky N, Brubaker PL, Auerbach AB, Joyner AL, et al. Glucose intolerance but normal satiety in mice with a null mutation in the glucagon-like peptide receptor gene. Nat Med 1996:21254–8.
[6] Baggio L, Kieffer TJ, Drucker DJ. Glucagon-like peptide-1, but not glucose-dependent insulinotropic peptide, regulates fasting glycemia and nonenteral glucose clearance in mice. Endocrinology 2000;141(10):3703–9.
[7] Schirra J, Sturm K, Leicht P, Arnold R, Goke B, Katschinski M. Exendin(9-39) amide is an antagonist of glucagon-like peptide-1(7- 36)amide in humans. J Clin Invest 1998;101(7):1421–30.
[8] Bose AK, Mocanu MM, Carr RD, Brand CL, Yellon DM. Glucagon-like peptide-1 (GLP-1) can directly protect the heart against ischemia/reperfusion injury. Diabetes 2005;54(1):146–51.
[9] Bose AK, Mocanu MM, Carr RD, Yellon DM. Glucagon like peptide-1 is protective against myocardial ischemia/reperfusion injury when given either as a preconditioning mimetic or at reperfusion in an isolated rat heart model. Cardiovasc Drugs Ther 2005;19(1):9–11.

[10] Gros R, You X, Baggio LL, Kabir MG, Sadi AM, Mungrue IN, et al. Cardiac function in mice lacking the glucagon-like peptide-1 receptor. Endocrinology 2003;144(6):2242–52.
[11] Read PA, Khan FZ, Dutka DP. Cardioprotection against ischaemia induced by dobutamine stress using glucagon-like peptide-1 in patients with coronary artery disease. Heart 2012;98(5):408–13.
[12] Nikolaidis LA, Mankad S, Sokos GG, Miske G, Shah A, Elahi D, et al. Effects of glucagon-like peptide-1 in patients with acute myocardial infarction and left ventricular dysfunction after successful reperfusion. Circulation 2004;109(8):962–5.
[13] Noyan-Ashraf MH, Momen MA, Ban K, Sadi AM, Zhou YQ, Riazi AM, et al. GLP-1R agonist liraglutide activates cytoprotective pathways and improves outcomes after experimental myocardial infarction in mice. Diabetes 2009;58(4):975–83.
[14] Noyan-Ashraf MH, Shikatani EA, Schuiki I, Mukovozov I, Wu J, Li RK, et al. A glucagon-like peptide-1 analogue reverses the molecular pathology and cardiac dysfunction of a mouse model of obesity. Circulation 2013;127(1):74–85.
[15] Lonborg J, Vejlstrup N, Kelbaek H, Botker HE, Kim WY, Mathiasen AB, et al. Exenatide reduces reperfusion injury in patients with ST-segment elevation myocardial infarction. Eur Heart J 2012;33(12):1491–9.
[16] Du X, Hu X, Wei J. Anti-inflammatory effect of exendin-4 postconditioning during myocardial ischemia and reperfusion. Mol Biol Rep 2014;41(6):3853–7.
[17] Salling HK, Dohler KD, Engstrom T, Treiman M. Postconditioning with cura-glutide, a novel GLP-1 analog, protects against heart ischemia-reperfusion injury in an isolated rat heart. Regul Pept 2012;178(1–3):51–5.
[18] Sattar N, Lee MMY, Kristensen SL, Branch KRH, Del Prato S, Khurmi NS, et al. Cardiovascular, mortality, and kidney outcomes with GLP-1 receptor agonists in patients with type 2 diabetes: a systematic review and meta-analysis of randomised trials. Lancet Diabetes Endocrinol 2021;9(10):653–62.
[19] Kristensen SL, Rorth R, Jhund PS, Docherty KF, Sattar N, Preiss D, et al. Cardiovascular, mortality, and kidney outcomes with GLP-1 receptor agonists in patients with type 2 diabetes: a systematic review and meta-analysis of cardiovascular outcome trials. Lancet Diabetes Endocrinol 2019;7(10):776–85.
[20] Hernandez AF, Green JB, Janmohamed S, D'Agostino RB, Sr., Granger CB, et al. Albiglutide and cardiovascular outcomes in patients with type 2 diabetes and cardiovascular disease (Harmony Outcomes): a double-blind, randomised placebo-controlled trial. Lancet 2018;392(10157):1519–29.
[21] Gerstein HC, Sattar N, Rosenstock J, Ramasundarahettige C, Pratley R, Lopes RD, et al. Cardiovascular and renal outcomes with efpeglenatide in type 2 diabetes. N Engl J Med 2021;385(10):896–907.
[22] Drucker DJ. The cardiovascular biology of glucagon-like peptide-1. Cell Metabol 2016;24(1):15–30.
[23] Ussher JR, Baggio LL, Campbell JE, Mulvihill EE, Kim M, Kabir MG, et al. Inactivation of the cardiomyocyte glucagon-like peptide-1 receptor (GLP-1R) unmasks cardiomyocyte-independent GLP-1R-mediated cardioprotection. Mol Metabol 2014;3(5):507–17.
[24] Wilson-Pérez HE, Chambers AP, Ryan KK, Li B, Sandoval DA, Stoffers D, et al. Vertical sleeve gastrectomy is effective in two genetic mouse models of glucagon-like peptide-1 receptor deficiency. Diabetes 2013;62(7):2380–5.
[25] O'Connell TD, Rodrigo MC, Simpson PC. Isolation and culture of adult mouse cardiac myocytes. Methods Mol Biol 2007:357271–96.
[26] Wong CK, Yusta B, Koehler JA, Baggio LL, McLean BA, Matthews D, et al. Divergent roles for the gut intraepithelial lymphocyte GLP-1R in control of metabolism, microbiota, and T cell-induced inflammation. 34. 10th ed. Cell Metab; 2022. p. 1514–31.
[27] Dobin A, Davis CA, Schlesinger F, Drenkow J, Zaleski C, Jha S, et al. STAR: ultrafast universal RNA-seq aligner. Bioinformatics 2013;29(1):15–21.
[28] Love MI, Huber W, Anders S. Moderated estimation of fold change and dispersion for RNA-seq data with DESeq2. Genome Biol 2014;15(12):550.
[29] Liao Y, Wang J, Jaehnig EJ, Shi Z, Zhang B. WebGestalt 2019: gene set analysis toolkit with revamped UIs and APIs. Nucleic Acids Res 2019;47(W1):W199–205.
[30] Tabula Muris C. Single-cell transcriptomics of 20 mouse organs creates a Tabula Muris. Overall c., Logistical c., Organ c., processing, Library p., et al Nature 2018;562(7727):367–72.
[31] Litvinukova M, Talavera-Lopez C, Maatz H, Reichart D, Worth CL, Lindberg EL, et al. Cells of the adult human heart. Nature 2020;588(7838):466–72.
[32] Kuppe C, Ramirez Flores RO, Li Z, Hayat S, Levinson RT, Liao X, et al. Spatial multi-omic map of human myocardial infarction. Nature 2022;608(7924):766–77.
[33] Hao Y, Hao S, Andersen-Nissen E, Mauck 3rd WM, Zheng S, Butler A, et al. Integrated analysis of multimodal single-cell data. Cell 2021;184(13):3573–87. e3529.
[34] Wolf FA, Angerer P, Theis FJ. SCANPY: large-scale single-cell gene expression data analysis. Genome Biol 2018;19(1):15.
[35] Ussher JR, Campbell JE, Mulvihill EE, Baggio LL, Bates HE, McLean BA, et al. Inactivation of the glucose-dependent insulinotropic polypeptide receptor improves outcomes following experimental myocardial infarction. Cell Metabol 2018;27(2):450–60.
[36] Kim M, Platt M, Shibasaki T, Quaggin S, Backx PH, Seino S, et al. GLP-1 receptor activation and Epac2 link atrial natriuretic peptide secretion to control of blood pressure. Nat Med 2013;19(5):567–75.
[37] Baggio LL, Yusta B, Mulvihill EE, Cao X, Streutker CJ, Butany J, et al. GLP-1 receptor expression within the human heart. Endocrinology 2018;159(4):1570–84.
[38] Andersen DB, Grunddal KV, Pedersen J, Kuhre RE, Lund ML, Holst JJ, et al. Using a reporter mouse to map known and novel sites of GLP-1 receptor expression in peripheral tissues of male mice. Endocrinology 2021;162(3).
[39] Miquerol L, Thireau J, Bideaux P, Sturny R, Richard S, Kelly RG. Endothelial plasticity drives arterial remodeling within the endocardium after myocardial infarction. Circ Res 2015;116(11):1765–71.
[40] Klein A, Bayrau B, Miao Y, Gu M. Isolation of endocardial and coronary endothelial cells from the ventricular free wall of the rat heart. JoVE 2020;158.
[41] Matheeussen V, Baerts L, De Meyer G, De Keulenaer G, Van der Veken P, Augustyns K, et al. Expression and spatial heterogeneity of dipeptidyl peptidases in endothelial cells of conduct vessels and capillaries. Biol Chem 2011;392(3):189–98.
[42] McLean BA, Wong CK, Kaur KD, Seeley RJ, Drucker DJ. Differential importance of endothelial and hematopoietic cell GLP-1Rs for cardiometabolic versus hepatic actions of semaglutide. JCI Insight 2021;6(22).
[43] Ban K, Kim H, Cho J, Diamandis E, Backx PH, Drucker DJ, et al. GLP-1(9-36) protects cardiomyocytes and endothelial cells from ischemia-reperfusion injury via cytoprotective pathways independent of the GLP-1 receptor. Endocrinology 2010;151(4):1520–31.
[44] Ban K, Noyan-Ashraf MH, Hoefer J, Bolz SS, Drucker DJ, Husain M. Cardioprotective and vasodilatory actions of glucagon-like peptide 1 receptor are mediated through both glucagon-like peptide 1 receptor-dependent and -independent pathways. Circulation 2008;117(18):2340–50.
[45] Siraj MA, Mundil D, Beca S, Momen A, Shikatani EA, Afroze T, et al. Cardioprotective GLP-1 metabolite prevents ischemic cardiac injury by inhibiting mitochondrial trifunctional protein-alpha. J Clin Invest 2020;130(3):1392–404.
[46] Baggio LL, Ussher JR, McLean BA, Cao X, Kabir MG, Mulvihill EE, et al. The autonomic nervous system and cardiac GLP-1 receptors control heart rate in mice. Mol Metabol 2017;6(11):1339–49.

[47] Hsieh J, Longuet C, Baker CL, Qin B, Federico LM, Drucker DJ, et al. The glucagon-like peptide 1 receptor is essential for postprandial lipoprotein synthesis and secretion. Diabetologia 2010;53(3):552–61.
[48] Ussher JR, Drucker DJ. Cardiovascular actions of incretin-based therapies. Circ Res 2014;114(11):1788–803.
[49] Holman RR, Bethel MA, Mentz RJ, Thompson VP, Lokhnygina Y, Buse JB, et al. Effects of once-weekly exenatide on cardiovascular outcomes in type 2 diabetes. N Engl J Med 2017;377(13):1228–39.
[50] Yamamoto H, Lee CE, Marcus JN, Williams TD, Overton JM, Lopez ME, et al. Glucagon-like peptide-1 receptor stimulation increases blood pressure and heart rate and activates autonomic regulatory neurons. J Clin Invest 2002;110(1):43–52.
[51] Lovshin JA, Barnie A, DeAlmeida A, Logan A, Zinman B, Drucker DJ. Liraglutide promotes natriuresis but does not increase circulating levels of atrial natriuretic peptide in hypertensive subjects with type 2 diabetes. Diabetes Care 2015;38(1):132–9.
[52] Helmstadter J, Frenis K, Filippou K, Grill A, Dib M, Kalinovic S, et al. Endothelial GLP-1 (Glucagon-Like peptide-1) receptor mediates cardiovascular protection by liraglutide in mice with experimental arterial hypertension. Arterioscler Thromb Vasc Biol 2020;40(1):145–58.
[53] Johnson RC, Crissman RS, DiDio LJ. Endocardial alterations in myocardial infarction. Lab Invest 1979;40(2):183–93.
[54] Dube KN, Thomas TM, Munshaw S, Rohling M, Riley PR, Smart N. Recapitulation of developmental mechanisms to revascularize the ischemic heart. JCI Insight 2017;2(22).
[55] Lonborg J, Kelbaek H, Vejlstrup N, Botker HE, Kim WY, Holmvang L, et al. Exenatide reduces final infarct size in patients with ST-segment-elevation myocardial infarction and short-duration of ischemia. Circ Cardiovasc Interv 2012;5(2):288–95.
[56] Woo JS, Kim W, Ha SJ, Kim JB, Kim SJ, Kim WS, et al. Cardioprotective effects of exenatide in patients with ST-segment-elevation myocardial infarction undergoing primary percutaneous coronary intervention: results of exenatide myocardial protection in revascularization study. Arterioscler Thromb Vasc Biol 2013;33(9):2252–60.
[57] Drucker DJ. Mechanisms of action and therapeutic application of glucagon-like peptide-1. Cell Metabol 2018;27(4):740–56.
[58] Robinson E, Cassidy RS, Tate M, Zhao Y, Lockhart S, Calderwood D, et al. Exendin-4 protects against post-myocardial infarction remodelling via specific actions on inflammation and the extracellular matrix. Basic Res Cardiol 2015;110(2):20.
[59] Hanif W, Alex L, Su Y, Shinde AV, Russo I, Li N, et al. Left atrial remodeling, hypertrophy, and fibrosis in mouse models of heart failure. Cardiovasc Pathol 2017:3027–37.
[60] Freed MS, Needleman P, Dunkel CG, Saffitz JE, Evers AS. Role of invading leukocytes in enhanced atrial eicosanoid production following rabbit left ventricular myocardial infarction. J Clin Invest 1989;83(1):205–12.
[61] Liu L, Gan S, Li B, Ge X, Yu H, Zhou H. Fisetin alleviates atrial inflammation, remodeling, and vulnerability to atrial fibrillation after myocardial infarction. Int Heart J 2019;60(6):1398–406.
[62] Begieneman MP, Emmens RW, Rijvers L, Woudstra L, Paulus WJ, Kubat B, et al. Myocardial infarction induces atrial inflammation that can be prevented by C1-esterase inhibitor. J Clin Pathol 2016;69(12):1093–9.
[63] Aronson D, Boulos M, Suleiman A, Bidoosi S, Agmon Y, Kapeliovich M, et al. Relation of C-reactive protein and new-onset atrial fibrillation in patients with acute myocardial infarction. Am J Cardiol 2007;100(5):753–7.
[64] Ridker PM, Everett BM, Thuren T, MacFadyen JG, Chang WH, Ballantyne C, et al. Antiinflammatory therapy with canakinumab for atherosclerotic disease. N Engl J Med 2017;377(12):1119–31.
[65] George MJ, Jasmin NH, Cummings VT, Richard-Loendt A, Launchbury F, Woollard K, et al. Selective interleukin-6 trans-signaling blockade is more effective than panantagonism in reperfused myocardial infarction. JACC Basic Transl Sci 2021;6(5):431–43.
[66] Broch K, Anstensrud AK, Woxholt S, Sharma K, Tollefsen IM, Bendz B, et al. Randomized trial of interleukin-6 receptor inhibition in patients with acute ST-segment elevation myocardial infarction. J Am Coll Cardiol 2021;77(15):1845–55.
[67] Ali S, Ussher JR, Baggio LL, Kabir MG, Charron MJ, Ilkayeva O, et al. Cardiomyocyte glucagon receptor signaling modulates outcomes in mice with experimental myocardial infarction. Mol Metabol 2014;4(2):132–43.

Fluorescent conjugated antibodies

Target	Source	Clone
CD16/32 (FC block)	Biolegend	93
CD31	Biolegend	390
CD45	Biolegend	30-F11
CD140a	Biolegend	APA5
F4/80	Biolegend	BM8
VEGFR2	Biolegend	89B3A5
LY6C	Biolegend	HK1.4

Primer list

Target	Source	Cat.
Ppia	Thermo Fisher Scientific	Mm02342430_g1
Glp1r	Thermo Fisher Scientific	Mm00445292_m1
Adgre1	Thermo Fisher Scientific	mm00802529_m1
Acta2	Thermo Fisher Scientific	Mm01546133_m1
Myl2	Thermo Fisher Scientific	Mm00440384_m1
Ly6g	Thermo Fisher Scientific	Mm04934123_m1
Cd3g	Thermo Fisher Scientific	Mm00438095_m1
Kdr	Thermo Fisher Scientific	Mm01222419_m1
Npr3	Thermo Fisher Scientific	Mm00435329_m1
Dpp4	Thermo Fisher Scientific	Mm00494538_m1
CD14	Thermo Fisher Scientific	Mm00438094_g1
Thbd	Thermo Fisher Scientific	Mm00437014_s1
Nfkb	Thermo Fisher Scientific	Mm00476361_m1
Flnc	Thermo Fisher Scientific	Mm00471824_m1
Tlr2	Thermo Fisher Scientific	Mm00442346_m1
Osm	Thermo Fisher Scientific	Mm01193966_m1
Lif	Thermo Fisher Scientific	Mm00434762_g1
Has1	Thermo Fisher Scientific	Mm03048195_m1
Cxcl3	Thermo Fisher Scientific	Mm01701838_m1
IL6	Thermo Fisher Scientific	Mm00446190_m1

Supplementary Table 1

Supplementary Table 2

	baseMean	log2FoldCh	lfcSE	stat	pvalue	padj
Cxcl2	192.9777	-2.5063	0.56842	-4.40923	1.04E-05	0.001941
Cxcl3	49.71432	-2.28227	0.512251	-4.45537	8.37E-06	0.001699
Il6	503.6481	-1.91753	0.534992	-3.58422	0.000338	0.024013
Lif	202.6682	-1.84314	0.524653	-3.51307	0.000443	0.02884
Osm	48.85174	-1.74317	0.50158	-3.47535	0.00051	0.03221
Ntrk2	50.051	-1.64708	0.489745	-3.36314	0.000771	0.041106
Ptges	56.91752	-1.38847	0.311765	-4.45359	8.44E-06	0.001699
Cd14	357.0668	-1.33345	0.378293	-3.52491	0.000424	0.028133
Themis2	64.48734	-1.28808	0.325057	-3.96262	7.41E-05	0.007877
Has1	384.9131	-1.18335	0.238108	-4.96981	6.70E-07	0.000223
Tnc	124.1411	-1.12653	0.273007	-4.12638	3.69E-05	0.004846
Tmem74b	34.22237	-1.10086	0.308693	-3.5662	0.000362	0.02467
Adgrg2	70.69035	-1.08562	0.318628	-3.40717	0.000656	0.037038
Ankrd34a	21.70639	-0.9776	0.294579	-3.31863	0.000905	0.046389
Ugdh	988.9519	-0.97109	0.198276	-4.89766	9.70E-07	0.000286
G0s2	270.0578	-0.94912	0.276107	-3.43749	0.000587	0.034813
Adamts8	221.0718	-0.94551	0.244926	-3.86041	0.000113	0.010739
Tlr2	129.8553	-0.92734	0.242221	-3.82847	0.000129	0.011811
Nkain1	237.3794	-0.89332	0.178681	-4.99953	5.75E-07	0.000201
Smim3	209.0281	-0.79612	0.188611	-4.22097	2.43E-05	0.00363
Dgat1	375.0605	-0.79364	0.211025	-3.76086	0.000169	0.014325
Hcn4	269.0024	-0.77982	0.208079	-3.74769	0.000178	0.014815
Fjx1	96.17038	-0.76044	0.170201	-4.4679	7.90E-06	0.00165
Cd24a	193.2078	-0.73618	0.153531	-4.79498	1.63E-06	0.000441
Gja4	175.9423	-0.72903	0.206694	-3.52712	0.00042	0.02804
Pdpn	222.6009	-0.71898	0.185637	-3.87304	0.000107	0.010271
1110008P1	167.1239	-0.69669	0.154325	-4.51445	6.35E-06	0.001506
Aldh1a2	168.8653	-0.68858	0.158854	-4.33466	1.46E-05	0.002551
Stx11	139.4301	-0.68398	0.173659	-3.93863	8.19E-05	0.008309
Mustn1	185.588	-0.68106	0.153186	-4.44599	8.75E-06	0.001734
Adamts4	1083.266	-0.68088	0.184268	-3.69508	0.00022	0.017276
Thbd	3483.184	-0.67863	0.165554	-4.09915	4.15E-05	0.005147
Sdc1	146.2154	-0.64281	0.169672	-3.78856	0.000152	0.013328
Chpf2	190.6668	-0.64186	0.155186	-4.13605	3.53E-05	0.00474
Ccnd1	685.7078	-0.63419	0.14077	-4.50515	6.63E-06	0.001526
Inka2	319.1884	-0.63381	0.175711	-3.60711	0.00031	0.022351
Phyhip	141.7389	-0.62015	0.167172	-3.70965	0.000208	0.016657
Tmem263	226.2319	-0.61454	0.170316	-3.60823	0.000308	0.022351
Cdr2l	236.0593	-0.59612	0.143379	-4.15762	3.22E-05	0.004496
Chst11	213.5961	-0.59602	0.167513	-3.55805	0.000374	0.025318
Gas2l1	413.5979	-0.5945	0.155391	-3.82585	0.00013	0.011856
Lrfn4	143.2889	-0.59127	0.142665	-4.14445	3.41E-05	0.004713
Prr33	280.4192	-0.5869	0.130303	-4.50415	6.66E-06	0.001526
Plvap	433.9088	-0.57559	0.137028	-4.20057	2.66E-05	0.003929
Ccrl2	187.9779	-0.57321	0.172527	-3.32243	0.000892	0.046231
Septin9	731.1176	-0.5624	0.142991	-3.93311	8.39E-05	0.008438

Cspg4	531.9554	-0.56177	0.146053	-3.84636	0.00012	0.011214
Chpf	342.9264	-0.54534	0.095906	-5.68623	1.30E-08	1.01E-05
S1pr3	482.2591	-0.5296	0.156717	-3.37935	0.000727	0.039551
Smad3	475.3812	-0.50467	0.106931	-4.71952	2.36E-06	0.000616
Lysmd4	139.061	-0.50276	0.14783	-3.40096	0.000672	0.037318
Slc25a10	143.9677	-0.49421	0.139349	-3.54657	0.00039	0.026313
Fabp5	449.308	-0.49198	0.118887	-4.13822	3.50E-05	0.00474
Socs2	912.6944	-0.48864	0.142367	-3.43226	0.000599	0.035334
Ankrd9	576.2244	-0.48699	0.123877	-3.93122	8.45E-05	0.00844
Slc45a3	367.2853	-0.47652	0.141456	-3.36864	0.000755	0.040456
Cmip	755.7306	-0.47398	0.111424	-4.25385	2.10E-05	0.003359
Tpd52	528.9814	-0.46343	0.138563	-3.34457	0.000824	0.04324
Alpl	638.2325	-0.4608	0.133462	-3.4527	0.000555	0.03366
Pgd	408.6539	-0.46026	0.130731	-3.52067	0.00043	0.028306
Zbtb7b	259.5576	-0.45549	0.134565	-3.38492	0.000712	0.038916
1810055G	185.6129	-0.45327	0.133228	-3.40216	0.000669	0.037318
Adamts15	301.4537	-0.45135	0.126389	-3.57113	0.000355	0.024462
Mob3c	366.2446	-0.44375	0.13264	-3.34555	0.000821	0.04324
Ppp1r14b	223.7455	-0.4402	0.127247	-3.45946	0.000541	0.033438
Fam219b	274.5706	-0.4362	0.125133	-3.48591	0.00049	0.031169
Zdhhc13	168.4108	-0.43296	0.131217	-3.29956	0.000968	0.048535
Zdhhc9	564.2633	-0.43122	0.103597	-4.16251	3.15E-05	0.004448
Tinf2	182.9621	-0.42201	0.121671	-3.46842	0.000524	0.032645
Map1b	392.7053	-0.41036	0.101202	-4.0549	5.02E-05	0.005948
Podxl	3508.867	-0.4064	0.108824	-3.73443	0.000188	0.015521
Tuba1a	806.7651	-0.39967	0.099962	-3.9982	6.38E-05	0.007184
Gpr146	1752.764	-0.3953	0.115841	-3.41242	0.000644	0.036863
Pgam1	414.4565	-0.35717	0.101864	-3.50634	0.000454	0.029292
Nfkb1	1127.922	-0.34347	0.100315	-3.42392	0.000617	0.035958
Txnrd1	2260.848	-0.33793	0.099123	-3.40919	0.000652	0.036983
Arl2bp	910.4413	-0.32199	0.093278	-3.45196	0.000557	0.03366
Esyt1	771.0722	-0.28913	0.087621	-3.29979	0.000968	0.048535
Nsmaf	840.2152	0.241649	0.070513	3.427014	0.00061	0.035805
Fabp3	19322.86	0.268864	0.078603	3.420539	0.000625	0.036047
Ubr2	2223.303	0.280319	0.083914	3.340553	0.000836	0.04355
Ctnnd1	1571.663	0.280593	0.082613	3.396453	0.000683	0.037691
Gcdh	850.389	0.320178	0.081036	3.951055	7.78E-05	0.008074
Susd6	2476.819	0.330204	0.087239	3.785039	0.000154	0.013406
Acer2	1147.97	0.336762	0.096533	3.488563	0.000486	0.03101
Ablim1	6758.946	0.337345	0.10159	3.320664	0.000898	0.046231
Peg13	938.1553	0.34279	0.067736	5.060694	4.18E-07	0.000163
Tango2	1624.815	0.365263	0.102002	3.580931	0.000342	0.024054
Fam49a	345.7112	0.380048	0.111912	3.395955	0.000684	0.037691
Crim1	738.7833	0.384699	0.105426	3.649006	0.000263	0.019755
Hand2os1	497.3466	0.402503	0.121547	3.311495	0.000928	0.047224
Perm1	4093.32	0.409878	0.119858	3.419686	0.000627	0.036047
Syne1	1820.492	0.430999	0.116207	3.708875	0.000208	0.016657

Ncapd3	238.0854	0.431922	0.12443	3.47121	0.000518	0.032461
Cdk12	387.0276	0.454849	0.131691	3.453906	0.000553	0.03366
Tbc1d8	172.7788	0.457192	0.131985	3.463963	0.000532	0.033036
Cdc42ep1	768.2492	0.458566	0.13409	3.419834	0.000627	0.036047
Ehbp1	1362.522	0.459571	0.115302	3.985791	6.73E-05	0.007507
Mxi1	531.3065	0.466239	0.12013	3.881119	0.000104	0.01008
Edrf1	254.82	0.474652	0.14329	3.312521	0.000925	0.047224
Asb14	853.525	0.476022	0.096594	4.928089	8.30E-07	0.000256
Pkp2	2127.706	0.476058	0.131395	3.623116	0.000291	0.021326
Abcb4	439.8057	0.478728	0.135977	3.52065	0.00043	0.028306
C130080G	2788.294	0.488835	0.134949	3.622371	0.000292	0.021326
Kcnip2	1631.569	0.494703	0.127131	3.891268	9.97E-05	0.009739
Mapt	1049.38	0.497985	0.13516	3.68441	0.000229	0.01791
Cldnd1	514.5716	0.498064	0.150846	3.301795	0.000961	0.048516
Lrrc2	4040.109	0.503693	0.115387	4.365254	1.27E-05	0.002342
Fam53c	353.4372	0.508556	0.147217	3.454455	0.000551	0.03366
Klhl24	2377.185	0.513294	0.149206	3.440171	0.000581	0.034625
Agtpbp1	1542.795	0.514653	0.099172	5.189479	2.11E-07	9.51E-05
Fam168a	1021.619	0.516437	0.151605	3.406462	0.000658	0.037038
Sirt1	315.9326	0.517589	0.155833	3.321437	0.000896	0.046231
Atp1a2	12096.52	0.521097	0.068853	7.568256	3.78E-14	5.02E-10
Tcea3	1013.11	0.522854	0.12736	4.105314	4.04E-05	0.005059
Fat1	716.8501	0.52554	0.138891	3.783835	0.000154	0.013406
Myo10	855.9055	0.535503	0.125167	4.2783	1.88E-05	0.003127
C1qtnf9	620.3993	0.550649	0.143392	3.840177	0.000123	0.011419
Ppme1	882.0523	0.554202	0.164453	3.36998	0.000752	0.040456
Mylip	353.3404	0.55517	0.13781	4.028517	5.61E-05	0.00654
Aff1	3031.041	0.558421	0.159098	3.509928	0.000448	0.029041
Cdk5rap1	149.9686	0.572058	0.173676	3.293823	0.000988	0.04935
Zbtb38	380.4799	0.574084	0.156529	3.667589	0.000245	0.018798
Etl4	666.4851	0.574349	0.144892	3.963993	7.37E-05	0.007877
Lmod3	649.8713	0.574501	0.14122	4.068121	4.74E-05	0.005723
Smyd2	912.4244	0.574566	0.17392	3.303615	0.000954	0.048386
Tcap	14916.35	0.576608	0.161185	3.577295	0.000347	0.024142
Filip1l	528.5943	0.590287	0.107877	5.471849	4.45E-08	2.57E-05
Klhl31	869.3161	0.59447	0.120061	4.951398	7.37E-07	0.000239
Kcnv2	183.4177	0.595777	0.162061	3.676258	0.000237	0.018277
Ahsg	359.4612	0.601345	0.167845	3.582752	0.00034	0.02402
Crhr2	224.9438	0.602929	0.141501	4.260947	2.04E-05	0.003297
Yipf7	1203.111	0.60576	0.153224	3.953437	7.70E-05	0.008057
Ttll1	513.4956	0.612689	0.163327	3.751304	0.000176	0.014695
Armc2	482.8657	0.616206	0.134756	4.57275	4.81E-06	0.001162
Cdk18	236.1299	0.616457	0.184336	3.344205	0.000825	0.04324
Gask1b	506.8281	0.622502	0.153476	4.056014	4.99E-05	0.005948
Rras2	977.7546	0.623141	0.163363	3.814463	0.000136	0.012166
Garem1	302.6655	0.625142	0.16559	3.77525	0.00016	0.013786
Yes1	355.4759	0.62999	0.157112	4.009816	6.08E-05	0.006968

Ing3	157.8105	0.637387	0.175558	3.63063	0.000283	0.021007
Adprhl1	4577.925	0.637929	0.167148	3.816555	0.000135	0.012145
Kalrn	334.2366	0.643186	0.184293	3.49001	0.000483	0.030992
Itprid2	828.6163	0.65092	0.164006	3.968874	7.22E-05	0.007862
Klf12	127.0168	0.662214	0.160913	4.115356	3.87E-05	0.004937
Stard13	820.8983	0.665388	0.148971	4.466558	7.95E-06	0.00165
Stard9	262.3371	0.673534	0.198023	3.401302	0.000671	0.037318
Map3k4	606.8064	0.682503	0.188427	3.622101	0.000292	0.021326
Rapgef2	694.5703	0.685802	0.160664	4.268552	1.97E-05	0.003226
Jph1	391.7603	0.686034	0.160349	4.278391	1.88E-05	0.003127
Ankrd1	55621.78	0.688726	0.194861	3.534454	0.000409	0.027411
Stard8	757.8237	0.695952	0.176462	3.943932	8.02E-05	0.00819
Nqo1	448.0096	0.697508	0.15534	4.490213	7.12E-06	0.001575
Myc	855.6413	0.703063	0.183537	3.830627	0.000128	0.011789
Otulin	410.6698	0.710265	0.19141	3.710697	0.000207	0.016657
Usp28	3667.869	0.717125	0.212847	3.369206	0.000754	0.040456
Tent5a	833.3879	0.719421	0.175718	4.094181	4.24E-05	0.00521
Fat4	163.7865	0.721726	0.196205	3.678423	0.000235	0.018228
Cyp4b1	355.1459	0.737754	0.206846	3.566685	0.000362	0.02467
Rnf115	595.9385	0.742354	0.222021	3.343626	0.000827	0.04324
Cavin4	1601.529	0.744528	0.173482	4.291683	1.77E-05	0.00302
Magi3	643.1369	0.745952	0.143944	5.18224	2.19E-07	9.51E-05
Pim1	1147.804	0.747789	0.172419	4.337056	1.44E-05	0.002551
Ppargc1a	2706.889	0.752296	0.216515	3.47456	0.000512	0.03221
Arhgap20	442.9441	0.757873	0.169068	4.482642	7.37E-06	0.001592
Tacc2	12324.42	0.763502	0.131846	5.790864	7.00E-09	7.15E-06
Dnajb4	4163.091	0.771032	0.194387	3.966482	7.29E-05	0.007876
Dipk2a	631.5337	0.772953	0.191177	4.043116	5.27E-05	0.0062
Zkscan5	278.9917	0.781134	0.205581	3.799646	0.000145	0.012831
Ankrd13a	706.164	0.782929	0.189866	4.123586	3.73E-05	0.004857
Thrb	338.789	0.798366	0.189124	4.221382	2.43E-05	0.00363
Ctbp2	286.6002	0.799003	0.154248	5.179992	2.22E-07	9.51E-05
Edn1	165.9228	0.803794	0.221414	3.630282	0.000283	0.021007
Tmem117	104.9424	0.813439	0.225598	3.605697	0.000311	0.022351
Fam161b	108.6461	0.823278	0.245315	3.356003	0.000791	0.042012
Tec	263.7649	0.82999	0.240903	3.445324	0.00057	0.034233
Apod	106.2877	0.835526	0.245062	3.409443	0.000651	0.036983
Sesn1	2509.751	0.835786	0.146435	5.707542	1.15E-08	9.51E-06
Kctd6	274.8891	0.840195	0.203448	4.129783	3.63E-05	0.004823
Tnik	383.2762	0.848687	0.176305	4.813758	1.48E-06	0.00041
Myocd	949.2842	0.849542	0.199825	4.251422	2.12E-05	0.003359
Hdac9	221.5866	0.860883	0.205578	4.187615	2.82E-05	0.00407
Tns3	964.6164	0.876652	0.218646	4.009464	6.09E-05	0.006968
A2m	69.38642	0.879638	0.233335	3.769847	0.000163	0.013908
Nos2	150.2368	0.883299	0.247263	3.572309	0.000354	0.024462
Nr1d1	1860.37	0.884227	0.222613	3.972043	7.13E-05	0.007822
Nes	958.9837	0.894631	0.205228	4.359215	1.31E-05	0.002375

Nuak1	1651.496	0.899636	0.232271	3.873224	0.000107	0.010271
Frmd6	823.8409	0.910615	0.217183	4.192842	2.75E-05	0.004021
Magix	220.8496	0.917208	0.223155	4.11018	3.95E-05	0.005001
Lbh	2833.139	0.924785	0.14373	6.434169	1.24E-10	2.75E-07
Dusp8	758.9466	0.952245	0.249461	3.817218	0.000135	0.012145
Fbp2	193.5798	0.954909	0.271523	3.516857	0.000437	0.028572
Thoc6	135.0564	0.963398	0.263836	3.651503	0.000261	0.019675
Rpl3l	2255.34	0.973322	0.176837	5.504047	3.71E-08	2.27E-05
Tiam2	400.7378	0.978923	0.260776	3.753892	0.000174	0.014636
Zbtb20	189.0859	0.982113	0.251885	3.899045	9.66E-05	0.009501
Csrp3	18151.23	0.989948	0.201038	4.924196	8.47E-07	0.000256
Hspa8	35170.5	1.009924	0.186683	5.409834	6.31E-08	3.36E-05
Lmod2	8972.038	1.019082	0.177063	5.755491	8.64E-09	8.20E-06
Cryab	33060.82	1.020616	0.230432	4.429134	9.46E-06	0.001848
Dusp27	1536.777	1.043165	0.302238	3.451471	0.000558	0.03366
Pcdh17	115.0406	1.056935	0.249823	4.230743	2.33E-05	0.003597
Cyfip2	2012.718	1.060095	0.192681	5.501804	3.76E-08	2.27E-05
Nrap	17655.92	1.062128	0.290743	3.653153	0.000259	0.01966
Myot	852.2515	1.074472	0.218128	4.925872	8.40E-07	0.000256
Relt	125.8216	1.07711	0.300415	3.585412	0.000337	0.024013
Itgb6	157.6642	1.086424	0.260658	4.168014	3.07E-05	0.004388
Hspb8	7912.783	1.107169	0.238626	4.639761	3.49E-06	0.000874
Dnaja4	3202.068	1.110654	0.228717	4.856025	1.20E-06	0.000338
Fhl1	6222.673	1.117892	0.19526	5.725131	1.03E-08	9.15E-06
Arid5b	766.1814	1.118791	0.172672	6.479284	9.22E-11	2.45E-07
Sh3rf2	149.3658	1.120709	0.306724	3.653803	0.000258	0.01966
Ier5	1974.247	1.12649	0.304285	3.702087	0.000214	0.016906
Cited2	500.2597	1.129173	0.220634	5.117865	3.09E-07	0.000127
Ifrd1	2203.753	1.175465	0.347089	3.386641	0.000708	0.038833
Irs2	1288.285	1.182716	0.231248	5.114487	3.15E-07	0.000127
Asb15	700.8608	1.1846	0.180034	6.579875	4.71E-11	1.56E-07
Hspa1l	225.526	1.206131	0.269172	4.480898	7.43E-06	0.001592
Bag3	6427.301	1.218497	0.328202	3.712648	0.000205	0.016657
Xirp2	15327.4	1.235391	0.32057	3.853732	0.000116	0.010958
Hspb1	12704.14	1.244581	0.363247	3.426269	0.000612	0.035805
Enah	6307.843	1.249935	0.362882	3.444466	0.000572	0.034233
Dnaja1	1454.644	1.252891	0.29088	4.307244	1.65E-05	0.002851
Fam13a	617.4635	1.314356	0.310401	4.234383	2.29E-05	0.003581
Pwwp3b	78.96076	1.466512	0.20658	7.099001	1.26E-12	7.79E-09
Flnc	55548.3	1.498393	0.354981	4.221048	2.43E-05	0.00363
Klhl41	3637.358	1.50599	0.380736	3.955474	7.64E-05	0.008052
2310002L0	523.5427	1.512557	0.239099	6.32606	2.52E-10	4.77E-07
Ccn2	9879.98	1.561169	0.283009	5.516315	3.46E-08	2.27E-05
Blm	33.68524	1.571353	0.379834	4.136947	3.52E-05	0.00474
Asb5	191.4414	1.589151	0.317316	5.008102	5.50E-07	0.000197
Xirp1	38264.15	1.604543	0.389335	4.12124	3.77E-05	0.004859
Habp2	133.9591	1.611277	0.349907	4.604869	4.13E-06	0.001015

Plk2	1079.702	1.617121	0.311491	5.191546	2.09E-07	9.51E-05
Adpgk	338.8436	1.624019	0.259709	6.253227	4.02E-10	6.68E-07
Prkag3	66.76159	1.654611	0.317098	5.217988	1.81E-07	8.97E-05
Dusp10	240.4208	1.699927	0.424418	4.005308	6.19E-05	0.007031
Gas2l3	51.82685	1.729995	0.425144	4.069197	4.72E-05	0.005723
Nle1	329.2817	1.745852	0.46289	3.771631	0.000162	0.013898
Klhl40	3304.325	1.839092	0.544594	3.376997	0.000733	0.039728
Sgo2a	79.34163	1.889778	0.527927	3.579622	0.000344	0.024054
Lmcd1	2314.748	2.054174	0.441749	4.650099	3.32E-06	0.000847
Scube2	176.8306	2.111108	0.346513	6.092429	1.11E-09	1.64E-06
Epn3	298.4474	2.120071	0.537463	3.944594	7.99E-05	0.00819
Myl3	45243.31	2.152271	0.43114	4.992051	5.97E-07	0.000203
Fer1l6	16.31263	2.177904	0.4842	4.497946	6.86E-06	0.001545
Abra	2258.57	2.270933	0.391247	5.804347	6.46E-09	7.15E-06
Aloxe3	31.54732	2.272398	0.513872	4.422112	9.77E-06	0.001859
Atf3	5166.885	2.279	0.611838	3.724844	0.000195	0.016023
Ccn1	7998.948	2.333944	0.411091	5.677443	1.37E-08	1.01E-05
Acta1	4536.929	2.352033	0.531943	4.421591	9.80E-06	0.001859
Ogdhl	2230.706	2.496784	0.497764	5.016002	5.28E-07	0.000195
Lrtm1	2830.649	2.539184	0.685447	3.704423	0.000212	0.016851
Vash2	52.93646	2.677759	0.457977	5.846926	5.01E-09	6.05E-06
Frat2	221.2832	2.677925	0.532249	5.03134	4.87E-07	0.000185
E2f8	24.07136	2.928996	0.52754	5.552183	2.82E-08	1.97E-05
Dnajb1	2117.099	2.976582	0.684511	4.34848	1.37E-05	0.00246
Myh7b	1537.346	3.189065	0.653633	4.878981	1.07E-06	0.000308
Gdnf	97.77592	3.468676	0.641255	5.409202	6.33E-08	3.36E-05
Otud1	4308.213	3.505268	0.586694	5.974605	2.31E-09	3.06E-06
Hspa1a	5025.03	4.730402	0.906826	5.21644	1.82E-07	8.97E-05
Hspa1b	5017.991	4.982983	1.041504	4.784411	1.71E-06	0.000456
Ush1c	50.86172	5.223033	1.337235	3.905845	9.39E-05	0.009307
Irx4	129.4407	5.231012	1.313899	3.981288	6.85E-05	0.007587
Myl2	72766.48	6.170849	0.875012	7.052301	1.76E-12	7.79E-09